On the modeling methods of small-scale piezoelectric wind energy harvesting

Liya Zhao[a] and Yaowen Yang[*]

School of Civil and Environmental Engineering, Nanyang Technological University, 50 Nanyang Avenue, 639798, Singapore

Abstract. The interdisciplinary research area of small scale energy harvesting has attracted tremendous interests in the past decades, with a goal of ultimately realizing self-powered electronic systems. Among the various available ambient energy sources which can be converted into electricity, wind energy is a most promising and ubiquitous source in both outdoor and indoor environments. Significant research outcomes have been produced on small scale wind energy harvesting in the literature, mostly based on piezoelectric conversion. Especially, modeling methods of wind energy harvesting techniques plays a greatly important role in accurate performance evaluations as well as efficient parameter optimizations. The purpose of this paper is to present a guideline on the modeling methods of small-scale wind energy harvesters. The mechanisms and characteristics of different types of aeroelastic instabilities are presented first, including the vortex-induced vibration, galloping, flutter, wake galloping and turbulence-induced vibration. Next, the modeling methods are reviewed in detail, which are classified into three categories: the mathematical modeling method, the equivalent circuit modeling method, and the computational fluid dynamics (CFD) method. This paper aims to provide useful guidance to researchers from various disciplines when they want to develop and model a multi-way coupled wind piezoelectric energy harvester.

Keywords: energy harvesting; wind energy; modeling; aeroelasticity; piezoelectric material

1. Introduction

The past decades have seen a dramatic rise in the interdisciplinary research area of "energy harvesting", which aims at sustaining the operation of off-grid wireless sensor networks (WSNs) and other low-power electronic devices. The ultimate objective of energy harvesting is to realize automatically self-powered WSNs and supply alternate power for small electronics, liberating them from the inconvenient replacement or recharge of the batteries, reducing the high cost of manual maintenance and eliminating the experimental pollution associated with the disposal of the chemical batteries. The energy harvesting techniques convert the ambient energy surrounding the electronic devices into electricity at a "small scale", usually at a level of milliwatt or even less. Due to advancement in electric circuit techniques, the size and power consumption of the electronics are greatly reduced, such that the "small-scaled" harvested energy is already sufficient to continuously run a low-power electronic device or to power a single duty cycle operation for high-power device.

Various energy sources are existing around the electronic system, like solar energy, thermo gradient (Strasser, Aigner *et al.* 2004), mechanical vibrations from machines and various human activities (Anton and Sodano 2007), and fluid energy like wind and ocean wave energy, etc. Among them, wind energy is a ubiquitous energy source existing in natural wind in the outdoor environments, flows in the indoor heating and ventilation air conditioning ducts, and flows generated from vehicle driving, etc. The technique of harvesting wind energy in large scale turbines has been developed very well, which can generate high-level power in kilo or megawatt in places where strong wind is available, like the offshore environment. A recent wind turbine model of V164-8.0 MW developed by "Vestas" is regarded as the world's biggest wind turbine, which has a 163 m diameter of rotor, a 21.124 m^2 swept area, and an 8.0 MW power output (Vestas V164-8.0 nacelle and hub). According to Global Wind Energy Council (GWEC), 4.46×10^{11} kWh of wind energy was generated worldwide in 2010, and around 2.5% of world electricity is supplied by wind power in these days (Global wind energy council, wind in numbers). Nevertheless, small scale fluid energy harvesting for powering small electronics has received only limited attention. As the power requirement of a single wireless sensor node is decreased down to mW level, some miniature designs have been reported to harvest small scale fluid energy at the level of mW or uW. Although the electromagnetic wind turbines perform well in large scale, miniaturization of such structures results in greatly reduced efficiency and increased manufacturing complexity with relatively large mechanical loss due to the relatively high viscous drag at low wind speeds.

Various small wind energy harvesters conduct power conversion based on seeking and enlarging flow-induced mechanical vibrations. The induced vibration energy can be

---

[*]Corresponding author, Associate Professor
  E-mail: cywyang@ntu.edu.sg
[a] Ph.D.
  E-mail: liyazhao@ntu.edu.sg

converted into electricity using various conversion mechanisms: electrostatic (Meninger, Mur-Miranda *et al.* 2001, Roundy, Wright *et al.* 2003, Torres and Rincón-Mora 2009, Sterken, Fiorini *et al.* 2004, Mitcheson, Miao *et al.* 2004), electromagnetic (El-Hami, Glynne-Jones *et al.* 2001, Glynne-Jones, Tudor *et al.* 2004, Elvin and Elvin 2011) and piezoelectric conversions (Roundy et al., 2003; Roundy and Wright 2004, Beeby, Tudor *et al.* 2006, Anton and Sodano 2007, Cook-Chennault, Thambi *et al.* 2008). Energy harvesting using piezoelectric materials has seen a dramatic rise in the past few years due to the high power density, ease to be integrated in micro-scale power generating systems like MEMS (Jeon, Sood *et al.* 2005, Dutoit, Wardle *et al.* 2005, Lu, Lee *et al.* 2004) and Nano-scale harvesters (Wang 2011), and simple configuration of piezoelectric energy harvesters, which usually take the form of a cantilever beam shown in Fig. 1. The energy conversion is realized using a special characteristic of the material called "piezoelectricity". Piezoelectricity was first discovered in 1880 by Pierre and Paul-Jacques Curie. They found out that when a mechanical stress was applied on certain crystals, electrical charges appeared, with the voltage being proportional to the applied mechanical stress. Vice versa, mechanical strain will occur when they are subjected to electric fields. These behaviors are labeled as direct and converse piezoelectric effects, respectively. Crystals displaying such behaviors include tourmaline, tourmaline, topaz, quartz, Rochelle salt and cane sugar (Piezoelectric materials (online)). Tremendous research interests have been spurred in designing efficient piezoelectric energy harvesters to harness kinetic energy from base vibrations (Erturk 2009, Tang, Yang *et al.* 2010, Castagnetti 2012, Karami 2012, Wang 2012, Harne and Wang 2013, Kim, Kim *et al.* 2011, Pellegrini, Tolou *et al.* 2013, Daqaq, Masana *et al.* 2014). In the area of small scale wind energy harvesting, most studies have also been conducted using piezoelectric conversion (Priya, Chen *et al.* 2005, Karami, Farmer *et al.* 2013, Zhao and Yang 2015a, b, Xiao and Zhu 2014, Abdelkefi 2012, Bryant 2012, Akaydin 2012, Hobeck 2014, Bibo 2014, Zhao 2015, Mccarthy, Watkins *et al.* 2016).

The rapidly growing interests in small scale wind energy harvesting have brought significant research outcomes in the literature. The advances have been reported in the review article of Truitt and Mahmoodi (2013) with a focus on active wind energy harvesting designs, and in the very recent and comprehensive review of Abdelkefi (2016) with a focus on the chronical progress in aeroelastic energy harvesting, which the readers are referred to as an introduction to this area. However, although there have been tremendous wind energy harvesting techniques, there is no comprehensive report on the modeling methods which play a greatly important role in properly designing harvester structures, accurately evaluating the wind power extraction performance, parameter optimizations, and efficiently enhancing harvesters' performance from both mechanical and circuit aspects. This paper presents a guideline on the modeling methods of small-scale wind energy harvesters. Different wind power extraction principles are first introduced, followed by detailed study on the modeling

methods which are classified into three categories: the mathematical modeling method, the equivalent circuit modeling method, and the computational fluid dynamics (CFD) method. Their merits, demerits and applicable circumstances are also compared and discussed. This paper aims to provide some guidance to researchers from various disciplines when they want to develop and model a three-way coupled, i.e., aero-electro-mechanically coupled, wind piezoelectric energy harvester.

2. Small-scale wind energy harvesting using piezoelectric materials

In order to provide a small scale but continuous power supply for small electronic devices like the WSNs, some research has been conducted to miniaturize the electromagnetic wind turbine into centimeter scale (Federspiel and Chen 2003, Rancourt, Tabesh *et al.* 2007, Myers, Vickers *et al.* 2007, Bansal, Howey *et al.* 2009, Howey, Bansal *et al.* 2011, Bressers, Vernier *et al.* 2010, 2011, Xu, Yuan *et al.* 2010, Park, Jung *et al.* 2012, Kishore, Coudron *et al.* 2013). Like the large scale wind turbines, these miniaturized wind turbines operate with the Faraday's law, consisting of rotating blades around a shaft and generating power with permanent magnets and coils through electromagnetic coupling.

When a traditional electromagnetic wind turbine is scaled down, system complexity and manufacturing difficulty will be increased. The power generation efficiency is lowered down due to the relatively high mechanical friction and viscous drag on the blades at low Reynolds numbers (Kwon 2010, Karami, Farmer *et al.* 2013). In view of the relatively high power density of piezoelectric transduction at small scale, some researchers have proposed designs of miniaturized windmill/turbine using piezoelectric transduction (Priya, Chen *et al.* 2005, Chen, Islam *et al.* 2006, Tien and Goo 2010, Karami, Farmer *et al.* 2013). In these designs, piezoelectric transducers are excited through impacts with the rotating shafts or blades in the wind, transferring the impact-induced vibration energy into electricity.

Recently, much effort has been made to harvest small wind energy through the aeroelasticity phenomena. When structures are subjected to wind flows, aeroelastic instabilities will occur, such as vortex-induced vibration, galloping, flutter, turbulence-induced vibration, wake galloping and buffeting. In the field of civil or aerospace engineering, this kind of instabilities is usually undesired. The famous Tacoma Narrows Bridge collapsed down in 1940 due to these aerodynamic instability phenomena. However, the energy of structural vibrations induced by aeroelastic instability can be beneficially converted to electricity using the vibration-based piezoelectric energy harvesting approach. In an aeroelastic energy harvester, piezoelectric transducers are not excited by blades as in a turbine, but directly interact with wind via a specific type of aeroelasticity. This paper focuses on small wind piezoelectric energy harvesting by exploiting such kinds of aeroelasticity phenomena.
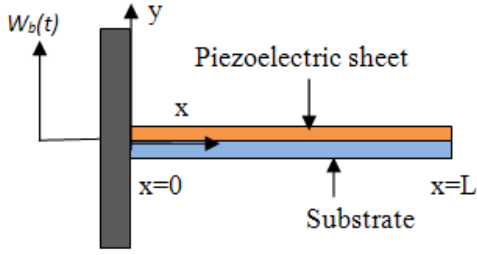
Fig. 1 A typical vibration piezoelectric energy harvester

In this section, the mechanisms and characteristics of different types of aeroelastic instabilities are presented, including the vortex-induced vibration, galloping, flutter, wake galloping and turbulence-induced vibration.

2.1 Vortex-induced vibration

Vortex-induced vibration (VIV) is one of the most classic aeroelastic instability phenomena. It is frequently observed in many engineering structures, such as tall buildings, slender chimneys, electric power lines, cables on bridges, marine cables, stacks, heat exchangers, offshore structures and other aerodynamic and hydrodynamic structures.

When a bluff body is subjected to a steady and uniform flow with high enough Reynolds number like 100, the effect of viscosity of the flow is only dominant near the boundary of the bluff body. The flow is separated by the bluff body, forming two sheer layers on each side, from which vortices are formed periodically (Williamson 1996, Païdoussis, Price *et al*. 2011, Facchinetti, De Langre *et al*. 2002, 2004). The creation process of the continuous alternating vortices in the downstream of the bluff body is called "vortex shedding". Fig. 2(a) gives a brief schematic of vortex shedding behind a bluff body while Fig. 2(b) shows the configuration of a typical VIV based piezoelectric energy harvester (Akaydin, Elvin *et al*. 2012, Dai, Abdelkefi et al., 2014a, b; Weinstein, Cacan *et al*. 2012, Abdelkefi, Hajj *et al*. 2012b). The behavior of vortex shedding has been extensively studied both theoretically and experimentally. For a thorough literature review, interested readers are referred to the review paper of Williamson (1996). The alternating vortices are shed to the wake at the "vortex shedding frequency" ω_f, defined as

$$\omega_f = 2\pi St \frac{U}{L} \qquad (1)$$

where l is the reference length scale which is generally taken as the cross-flow frontal dimension of the bluff body; U is the wind velocity; and St is the Strouhal number. For some section shapes commonly employed in civil structures, the corresponding Strouhal numbers are given in Fig. 3, in the limit of large Reynolds numbers (say 1000) (Païdoussis, Price *et al*. 2011).

Under the action of vortex shedding, the bluff body will undergo, usually periodic, oscillations, which is the so called VIV, resulting in a complex interaction between the bluff body and the vortices. Two main features of VIV are

summarized by Barrero-Gil, Pindado *et al*. (2012). Firstly, there is a lock-in regime of wind speed, where the vortex shedding frequency is kept synchronized with the oscillation frequency associated with large amplitude oscillations; secondly, hysteresis appears in the displacement response of a cylinder undergoing VIV. More detailed research on VIV phenomenon has been reviewed by Sarpkaya (2004) and Williamson and Govardhan (2004). Typically, the range of wind speed giving significant vortex-induced vibrations for effective power generation is narrow, which remains a main constraint for VIV-based energy harvesting. A typical response curve of oscillation amplitude versus wind speed for VIV in a steady flow is depicted in Fig. 4.

(a) Vortex shedding
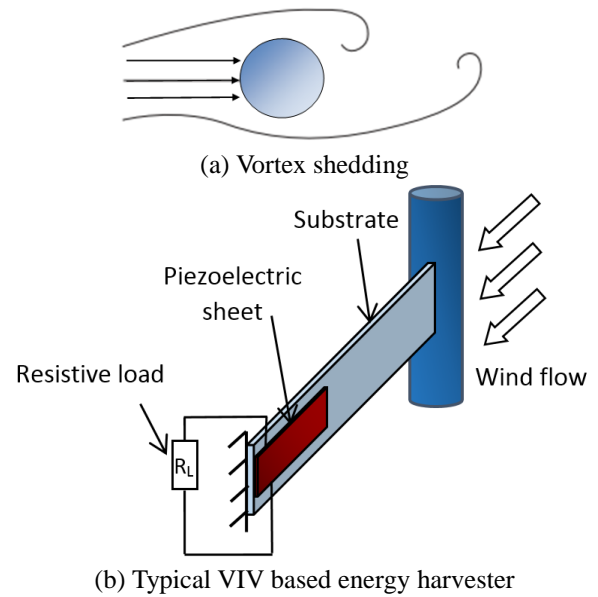

(b) Typical VIV based energy harvester

Fig. 2 Schematic of vortex shedding and a typical VIV based energy harvester
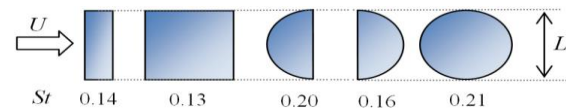

Fig. 3 Strouhal number for some commonly employed section shapes in civil structures at large Reynolds number
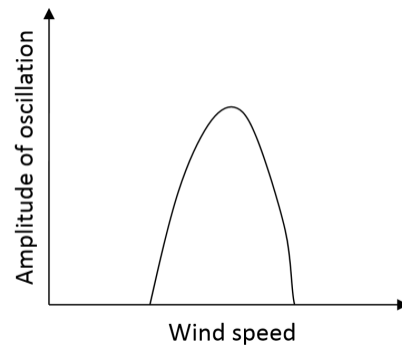

Fig. 4 Typical response of amplitude of oscillation versus wind speed for VIV
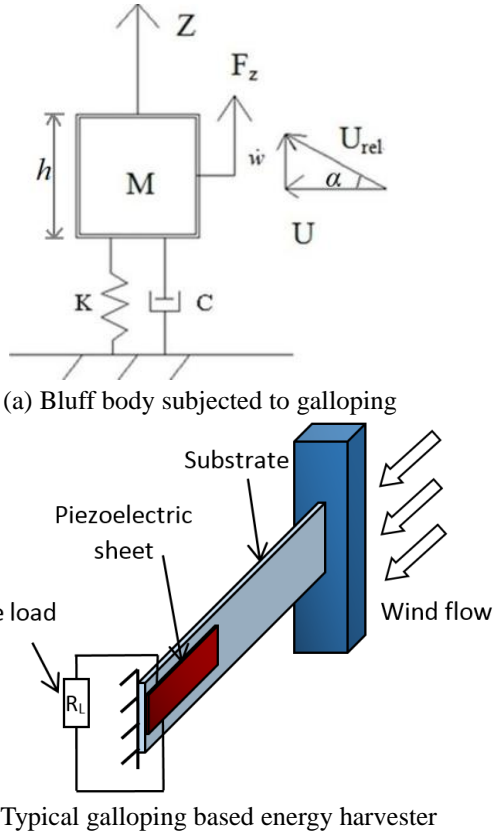
(a) Bluff body subjected to galloping

(b) Typical galloping based energy harvester

Fig. 5 Schematic of a bluff body subjected to galloping and a typical galloping based energy harvester

2.2 Galloping

Translational galloping is a self-excited phenomenon giving rise to large amplitude oscillations of bluff body when subjected to wind flows. However, it is not really "self-excited", but the governing equation of the vibration due to galloping can be written in a way that the input aerodynamic force is hidden, making the motion seem to be self-excited.

Assume that a bluff body is mounted on a spring as shown in Fig. 5(a). Wind flows from the right to the left with a velocity of U. The governing equation of the galloping motion can be written as

$$M\ddot{w} + C\dot{w} + Kw = F_Z \tag{2}$$

where w is the vertical position of the mass center of the bluff body; M is the mass of the bluff body; C is the damping coefficient; K is the stiffness of the spring and F_z is the aerodynamic force. The overdot denotes differentiation with respect to time t. F_z depends on the geometry properties of the bluff body, the wind velocity U and the bluff body vibration velocity $\dot{w}$. F_z can be expressed as a polynomial function of the angle of attack α, and for simplicity, it can be written as

$$F_Z = XU^2(A\alpha - B\alpha^3) \tag{3}$$

where X is a constant related to the air density and the geometry properties of the bluff body, and A and B are both positive empirical coefficients. Quasi-steady aerodynamics is applicable here because the frequency of vibration caused by galloping is low enough (Païdoussis, Price *et al*. 2011). If the bluff body undergoes only translational oscillation without rotation, the angle of attack α can be expressed as

$$\alpha = \frac{\dot{w}}{U} \tag{4}$$

Substituting Eqs. (3) and (4) into Eq. (2), and dividing both sides of Eq. (2) by M yields

$$\ddot{w} + (2\varsigma\omega_n - \frac{XA}{M}U + \frac{XB}{MU}\dot{w}^2)\dot{w} + \omega_n^2 w = 0 \tag{5}$$

where ζ is the damping ratio and ω_n is the natural frequency of the system. In such a way as in Eq. (5), the aerodynamic force can be considered as an effective damping and is "hidden" as mentioned before.

First, the bluff body is set still. With any small disturbance, $\dot{w}$ is arbitrarily small, so we only need to consider the first two terms of the damping in the brackets in Eq. (5). For sufficiently small U, the term $(2\zeta\omega_n\text{-}XAU/M)$ is positive, thus the damping of the system is positive and the oscillations will be damped to the zero equilibrium. When the wind velocity increases and exceeds a certain value, the term $(2\zeta\omega_n\text{-}XAU/M)$ will become negative, giving rise to self-excited oscillation of the bluff body, which is usually called a Horf bifurcation. When $\dot{w}$ is large enough due to the increasing amplitude of oscillation, the third term of damping expression $(XB/MU)\dot{w}^2$ should be taken into account, making the overall damping non-negative. When the overall damping reaches zero, the vibration amplitude will be stable and the limit cycle oscillation will occur. Due to the self-excited and self-limiting characteristics of galloping, it is deemed a prospective energy source for energy harvesting. Fig. 5(b) shows the configuration of a typical galloping based piezoelectric energy harvester (Zhao, Tang *et al*. 2012, 2013, 2014a, Zhao and Yang 2015a, Abdelkefi, Hajj *et al*. 2012c, 2013a, b, Bibo and Daqaq 2014, Ewere, Wang *et al*. 2014, Yan and Abdelkefi 2014).

Fig. 6 shows the typical response curves of galloping amplitude versus wind speed. The form of responses mainly depends on the cross section shape of the bluff body and the flow condition, i.e., smooth flow or turbulent flow. Besides the supercritical response that is self-excited as discussed above, there exists the subcritical galloping response (Fig. 6(c)), where a large initial perturbation is necessary to induce galloping. This type of galloping is a feasible choice for energy harvesting if external perturbations are available and the ambient wind speed is decreasing. However, if these conditions are not satisfied, the self-excited supercritical galloping is the superior choice. Some cross sections also display a hysteresis region as shown in Fig. 6(b).

(a) Supercritical bifurcation

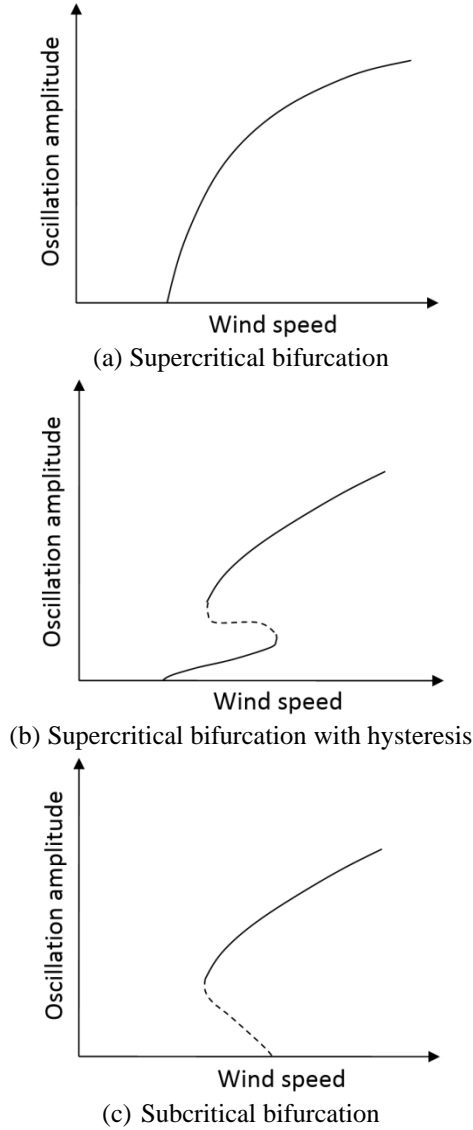(b) Supercritical bifurcation with hysteresis

(c) Subcritical bifurcation

Fig. 6 Typical response of amplitude of oscillation versus wind speed for galloping

The criterion for self-excited galloping (i.e., without the requirement of an external perturbation) is expressed as (Den Hartog 1956)

$$\frac{\partial C_{Fz}}{\partial \alpha} > 0 \tag{6}$$

where C_{Fz} is the total aerodynamic force coefficient in the direction normal to the incoming flow (Païdoussis, Price *et al.* 2011).

2.3 Flutter

The concept of exploiting flutter oscillation in a mill wing as a possible power generator can be traced back to several decades ago (McKinney and DeLaurier 1981, Schmidt 1985, 1992, Jones, Davids *et al.* 1999). Flutter instability was initially studied in the field of aeronautics. The flutter instabilities of aircraft wings and empennage structures are common examples of this type of phenomena,

which can cause severe damage to the flight vehicles.

There are several forms of flutter instabilities, such as the cross-flow flutter of a cantilever or a flexible belt (De Marqui, Erturk *et al.* 2010, Humdinger Wind Energy, Windbelt Innovation), the flutter of a cantilevered plate in axial flow (Huang 1995, Tang, Yamamoto *et al.* 2003), and the flutter of an airfoil with coupled torsion and bending motions (Theodorsen 1934, Peters, Karunamoorthy *et al.* 1995, Hodges and Pierce 2002). All the above types of flutter have been employed to harvest the flow energy. Among these types of flutter, the flutter of an airfoil has been studied with the greatest enthusiasm (Zhu 2011, Zhu and Peng 2009, Zhu, Haase *et al.* 2009). In this section, we focus on the mechanism of the aeroelastic flutter of an airfoil which undergoes pitch and plunge motions simultaneously.

A formal definition of aeroelastic flutter is described in the book of Hodges and Pierce (2002) as: a dynamic instability of a flight vehicle associated with the interaction of aerodynamic, elastic, and inertial forces. It is a self-excited oscillatory motions caused by the aerodynamics forces coupling with the natural modes of vibration. The magnitude of oscillation increases with the wind speed once it surpasses the critical value, which is the so called flutter speed. Typical response curves of amplitude versus wind speed for flutter in a steady flow is depicted in Fig. 7. As shown in the responses, flutter amplitude can either infinitely increase with wind speed associated with supercritical bifurcation, or gradually diminish or even vanish at a cut-out wind speed associated with subcritical bifurcation, depending on the parameters of the structural system (Bryant, Shafer *et al.* 2012, Abdelkefi, Nayfeh *et al.* 2012b). A typical section subject to aeroelastic flutter is an airfoil, with pitch and plunge modes as shown in Fig. 8(a).

Fig. 8(b) shows the configuration of a typical energy harvester based on flutter (Bryant, Wolff *et al.* 2011, Bryant, Shafer *et al.* 2012, Bryant, Tse *et al.* 2012, Bryant, Schlichting *et al.* 2013, Bryant, Pizzonia *et al.* 2014, Abdelkefi, Hajj *et al.* 2012d, e, Zhu 2011, Zhu and Peng 2009, Zhu, Haase *et al.* 2009). Flutter occurs when the two modal frequencies of the corresponding torsion and bending modes coalesce with each other. Since it results from the convergence of two structural modes, it is also referred to as the coupled mode flutter (Hodges and Pierce 2002). The critical condition at the stability boundary is called the flutter boundary, at which the corresponding wind speed is called the flutter speed. Below the flutter speed, the system will always return to stable status because the airflow provides positive damping. Above the flutter speed, however, any small perturbations can cause exponentially increased amplitude of oscillations due to the flow induced negative damping. Finally, because of the nonlinearity in the system (material, geometric or aerodynamic nonlinearity), the amplitude of oscillation will become constant and the system undergoes the limit cycle oscillation.

From a quantitative perspective, the flutter boundary depends on the real and imaginary parts of the two complex conjugate pairs of eigenvalues, e.g., $\Gamma_1 \pm i\Omega_1$ and $\Gamma_2 \pm i\Omega_2$, corresponding to the bending and rotation modes using the

famous *p* method (Hodges and Pierce 2002). The negative of the real component -Γ stands for the modal damping; while the imaginary component Ω stands for the modal frequency. When the wind speed increases from zero, the values of the two imaginary components gradually approach each other, while the values of the real components are both negative.
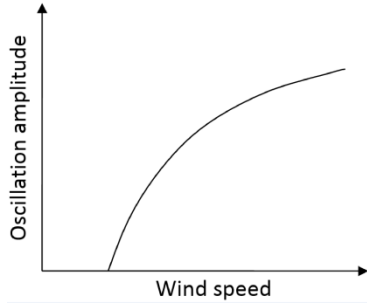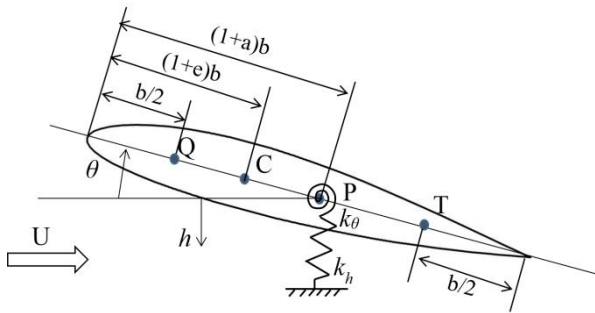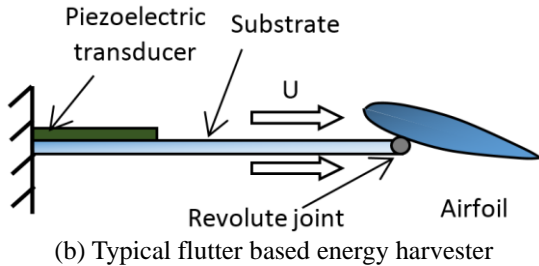

(a) Supercritical bifurcation
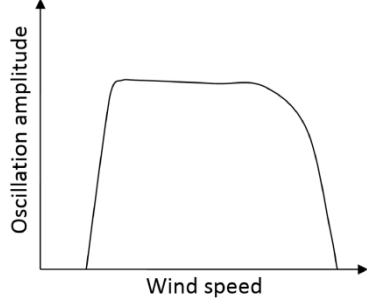
(b) Subcritical bifurcation

Fig. 7 Typical responses of amplitude of oscillation versus wind speed for flutter

(a) Typical flapping wing undergoing pitch and plunge motions, i.e., θ and h

(b) Typical flutter based energy harvester

Fig. 8 Schematic of a typical flapping wing and a typical flutter based energy harvester
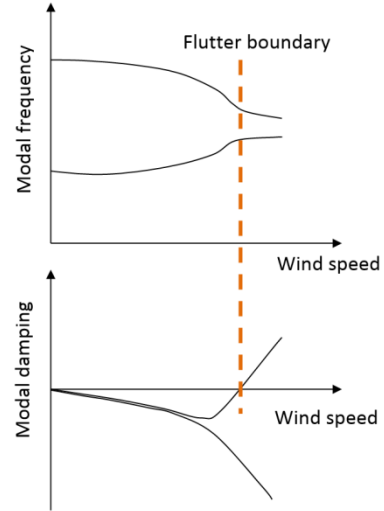

Fig. 9 Typical variations of modal frequency and modal damping with wind speed

At the flutter boundary, the two imaginary components coalesce with each other but do not fully converge, while one of the two real components becomes zero. This point represents that the system no longer undergoes decaying damped oscillations under external perturbations, but is associated with growing amplitude oscillations. Fully coupled pitch-plunge oscillations occur, with the flow energy being converted into vibration energy. Fig. 9 shows the typical variations of modal frequency and modal damping with wind speed obtained using the *p* method.

2.4 Wake-induced oscillations

Wake-induced oscillations occur to pairs or groups of cylinders, when one or more cylinders are positioned in the wake of one windward cylinder. In engineering applications, this type of oscillations frequently happen to bundles of transmission lines, twin cables in the offshore structures, twin slender chimneys and arrays of heat-exchanger tubes, etc. The aerodynamic characteristics of the vibrations of the leeward cylinder (or cylinders) depend significantly on the arrangement of cylinders as well as the Reynolds number. Specifically, for twin cylinders, the spacing ratio *L/D*, with *L* indicating the distance between centers of cylinders and *D* being the diameter of the cylinder, is a key parameter that determines the characteristics of wakes and the induced vibrations.

(1) Interference galloping
Interference galloping occurs to twin cylinders closely located to each other, say, *L/D*≤3. As indicated by Ruscheweyh (1983), the interference galloping is a self-excited oscillation phenomenon, with the onset wind speed depending on several factors like mass-damping parameter, spacing of the cylinders and the specific interference galloping criterion. It was found that large amplitude oscillation of the leeward cylinder is induced by the accelerated gap flow and the surrounding accelerated outside flow (Shiraishi 1986). The initial vertical position of

the leeward cylinder relative to the windward one has a great influence on the dynamic characteristics.

(2) Wake galloping

Wake galloping also occurs to twin cylinders, which are often two circular cylinders of tandem arrangement (i.e., the windward cylinder lies along the centerline of the wake of the leeward cylinder), causing periodic oscillations of the leeward cylinder due to the wake interference. It is found that wake galloping can happen when L/D is between 1.5 and 6 (Tokoro, Komatsu *et al.* 2000). A schematic of wake galloping is shown in Fig. 10(a). The amplitude of wake galloping also increases unlimitedly with wind speed (Jung and Lee 2011), like the case of galloping shown in Fig. 6. Oscillations due to wake galloping have been successfully utilized to harvest the flow energy by several researchers (Jung and Lee 2011, Hobbs and Hu 2012, Abdelkefi, Scanlon *et al.* 2013). Due to the complexity of the wakes and the mutual effects of numerous parameters, these studies were mainly conducted via experimental methods.

(3) Wake- induced flutter

Wake-induced flutter occurs to the twin or groups of cylinders with large gaps, i.e., L/D=10~20 (Tokoro, Komatsu *et al.* 2000). A typical engineering example of this type of instability is the coupled movement of bundles of transmission conductors. Unlike galloping which is a one degree-of-freedom (1DOF) damp controlled instability, wake-induced flutter is governed by aerodynamic stiffness and requires at least two degree-of-freedom (2DOF) (Païdoussis, Price *et al.* 2011). Near the instability boundary, the two modes (the in-plane and out-of-plane modes) coalesce with each other, like the case of flutter, which gives it the name "wake-induced flutter". The trajectory of the vibration of a flexibly mounted leeward cylinder in the wake of a fixed windward cylinder is usually an ellipse shown in Fig. 10(b). Due to its potential to cause serious damages in engineering applications with its associated large amplitude of vibration, extensive experimental and theoretical studies have been conducted to analyze the dynamic characteristics (Païdoussis, Price *et al.* 2011). Up to now, this kind of wind induced instability has not been applied in energy harvesting studies. However, it is definitely a feasible alternative to extract the flow energy.

2.5 Turbulence-induced vibration

The above mentioned aeroelastic instabilities, including VIV, galloping, flutter and wake galloping, have one important common feature that their occurrences require the wind speed to be beyond the critical wind speed, i.e., the cut-in or onset wind speed. Turbulence-induced vibration (TIV), however, is unavoidable as long as the turbulent flow is in contact with an elastic structure (Au-Yang 2001, Hobeck 2014). This makes it an advantageous alternative instability source for energy harvesting purpose.

TIV frequently occurs to natural vegetations like tree leaves, wheat and grass. Inspired by the motions of grass under turbulent flow, Hobeck and Inman (2012b) developed a "piezoelectric grass harvester", which consists of an array of vertically erected piezoelectric cantilevers. These cantilevers undergo vigorous vibrations under proper

turbulent flow conditions, converting the induced strain energy into electricity through piezoelectric transduction.

Large amplitude oscillations induced by turbulence occur at the wind speed where the vortex shedding frequency matches the fundamental frequency of the elastic structure to induce resonance (Akaydin, Elvin *et al.* 2010a, b, Hobeck and Inman 2012b). Therefore, there exists a critical wind speed for the maximum amplitude of displacement. Yet the amplitude will never be zero when the wind speed is below or beyond this critical value. Fig. 11 shows the typical response of the amplitude of oscillation versus wind speed for TIV.

3. Mathematical modeling - Part I: electromechanical model

Various modeling methods for aeroelastic piezoelectric energy harvesters have been proposed in the literature. Generally, these methods can be classified into three categories: the mathematical modeling method, the equivalent circuit modeling method, and the computational fluid dynamics method. This section presents the mathematical modeling method for aeroelastic piezoelectric energy harvesters.

(a) Schematic of wake galloping of parallel cylinders
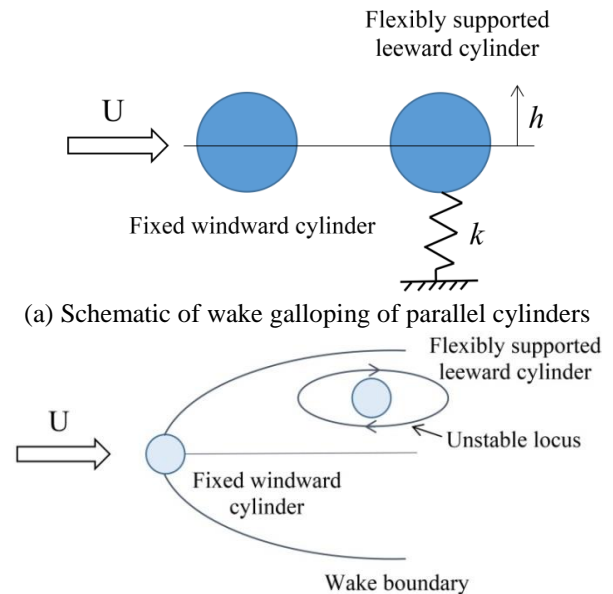
(b) Typical trajectory of the leeward cylinder during wake-induced flutter
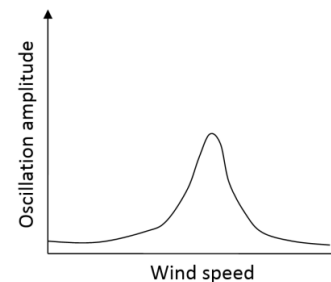
Fig. 10 Weak galloping phenomenon

Fig. 11 Typical response of amplitude of oscillation versus wind speed for TIV

The coupling effects for aeroelastic piezoelectric energy harvesters contain two parts: the electromechanical coupling between the piezoelectric material and the mechanical structure, and the aeroelastic coupling between the mechanical structure and the incoming flow. Therefore, the mathematical model for aeroelastic piezoelectric energy harvesters also includes two parts: the electromechanical model and the aerodynamic model.

Electromechanical modeling methods have been widely studied for vibration-based piezoelectric energy harvesting. For aeroelastic piezoelectric energy harvesting, the analysis of the electromechanical coupling is based on the vibration energy harvesting techniques. Electromechanical models include the uncoupled and coupled 1DOF model, which is also called the lumped parameter model, the uncoupled and coupled distributed parameter model, and the approximate distributed parameter model (Reyleigh-Ritz approach based model). An electromechanical model generally includes two equations: the mechanical equation, and the electrical circuit equation. Erturk and Inman (2008b) discussed the issues in the electromechanical modeling of vibration-based piezoelectric energy harvesters. The existing models are presented in this section.

3.1 Lumped parameter model

(1) Uncoupled 1DOF model

Representing the mechanical domain as a mass-spring-damper system (1DOF model) can obtain useful fundamental insights of the energy harvester. This method was firstly applied to electromagnetic generators by Williams and Yates (1996). Considering a magnetic seismic mass moving inside a coil as the microelectric generator, the governing equation for this system is

$$m\ddot{z} + c\dot{z} + kz = -m\ddot{y} \tag{7}$$

where y is the base excitation; z is the displacement of the seismic mass m relative to the base excitation; k is the spring constant; and c is the total damping, which contains the mechanical damping and electrical damping induced by electromagnetic energy harvesting. Regarding the coupling effect as viscous damping is suitable for electromagnetic energy harvesting, but is not proper for piezoelectric energy harvesting, since the effect of piezoelectric coupling is more sophisticated than the simple viscous damping effect.

(2) Coupled 1DOF model

Dutoit, Wardle *et al.* (2005) proposed a coupled 1DOF model for a piezoelectric energy harvester working in the 33 mode. The governing equations are

$$\ddot{w} + 2\zeta_m\omega_n\dot{w} + \omega_n^2w - \omega_n^2d_{33}v = -\ddot{w}_B \tag{8}$$

$$R_{eq}C_P\dot{v} + v + m_{eff}R_{eq}d_{33}\omega_n^2\dot{w} = 0 \tag{9}$$

where w_B is the base displacement; w is the displacement of the proof mass relative to the base; v is the voltage output; m_{eff} is the effective mass; ζ is the mechanical damping ratio; ω_n is the undamped natural frequency; and C_P is the

capacitance of the piezoceramic. The backward coupling effect of the electric output is treated as $-\omega_n^2d_{33}v$, making the model a "coupled" one. Eq. (8) is the mechanical equation of motion, and Eq. (9) is the electrical circuit equation.

(3) 1DOF correction factor

A piezoelectric energy harvester usually consists of a cantilever beam connected with a tip mass (proof mass) at the free end. Erturk and Inman (2008b) showed that if the proof mass of the harvester is not much larger than the mass of the cantilevered beam, the uncoupled and coupled 1DOF models underestimate the power output due to the inaccurate consideration of the contribution of the distributed beam mass to the excitation amplitude. The uncoupled 1DOF model should be modified with correction factors as

$$m\ddot{z} + c\dot{z} + kz = -\mu_1m\ddot{y} \tag{10}$$

$$m\ddot{z} + c\dot{z} + kz = -\kappa_1m\ddot{y} \tag{11}$$

where μ_1 and κ_1 are the correction factors for transverse vibrations and longitudinal vibrations, respectively, given by

$$\mu_1 = \frac{(M_t/mL)^2 + 0.603(M_t/mL) + 0.08955}{(M_t/mL)^2 + 0.4637(M_t/mL) + 0.05718} \tag{12}$$

$$\kappa_1 = \frac{(M_t/mL)^2 + 0.7664(M_t/mL) + 0.2049}{(M_t/mL)^2 + 0.6005(M_t/mL) + 0.161} \tag{13}$$

where M_t is the proof mass; m is the distributed mass of the cantilever and L is the cantilever length. Moreover, applying κ_1 to the coupled 1DOF model, the mechanical equation of motion Eq. (8) becomes

$$\ddot{w} + 2\zeta_m\omega_n\dot{w} + \omega_n^2w - \omega_n^2d_{33}v = -\kappa_1\ddot{w}_B \tag{14}$$

The subscript 1 stands for the fundamental mode.

3.2 Distributed parameter model

In order to take the effects of higher vibration modes into account, Erturk and Inman (2008a) presented a distributed parameter model for a unimorph vibration energy harvester without the proof mass. The governing mechanical equation is

$$\frac{\partial^2}{\partial x^2}\left[YI\frac{\partial^2 w_{rel}(x,t)}{\partial x^2}\right] + c_sI\frac{\partial^5 w_{rel}(x,t)}{\partial x^4\partial t} + c_a\frac{\partial w_{rel}(x,t)}{\partial t} + m\frac{\partial^2 w_{rel}(x,t)}{\partial t^2} \\ + \theta v(t)\left[\frac{d\delta(x-x_1)}{dx} - \frac{d\delta(x-x_2)}{dx}\right] = -m\frac{\partial^2 w_b(x,t)}{\partial t^2} - c_a\frac{\partial w_b(x,t)}{\partial t} \tag{15}$$

where YI is the average bending stiffness; I is the equivalent area moment of inertia of the composite cross section; L is the length of the beam; m is the mass per unit length; θ is the electromechanical coupling coefficient; c_s and c_a are the strain rate damping coefficient and viscous air damping coefficient, respectively; w_b and w_{rel} are the base excitation and the deflection relative to the base motion, respectively; v is the output voltage of the energy harvester; and $\delta(x)$ is

the Dirac delta function.

Substituting the modal expansion of the relative deflection given by $w_{rel}(x,t) = \sum_{r=1}^{\infty} \phi_r(x)\eta_r(t)$, the coupled mechanical equation in modal coordinates can be obtained as

$$\ddot{\eta}_r(t) + 2\zeta_r\omega_r\dot{\eta}_r(t) + \omega_r^2\eta_r(t) + \chi_r v(t) = -\frac{\partial^2 w_b(x,t)}{\partial t^2}\left(m\int_0^L \phi_r(L)dx\right) \quad (16)$$

Considering the simple electrical circuit consisting of a resistive load only, the coupled electrical circuit equation is

$$\frac{v(t)}{R_l} + C_p\dot{v}(t) - \sum_{r=1}^{\infty}\varphi_r\dot{\eta}_r(t) = 0 \quad (17)$$

In Eqs. (16) and (17), $\phi_r(x)$ and $\eta_r(t)$ are the modal eigenfunction and modal coordinate, respectively, and χ_r and φ_r are both electromechanical coupling coefficients.

3.3 Rayleigh-Ritz type of approximate distributed parameter model

For harvesters with more complicated structures than a uniform cantilever beam, the deviation of accurate analytical solutions would be either more cumbersome or impossible. An approximate coupled distributed parameter model based on the Rayleigh-Ritz method was proposed by several researchers (Dutoit, Wardle *et al.* 2005, Sodano, Park *et al.* 2004). Elvin and Elvin (2009b) presented the Rayleigh-Ritz type coupled electromechanical equations given by

$$\mathbf{M\ddot{r}} + \mathbf{C\dot{r}} + \mathbf{Kr} - \mathbf{\Theta v} = -\ddot{w}_b\left(\int_0^L \mathbf{m\varphi}(x)dx + M_t\mathbf{\varphi}(L)\right) \quad (18)$$

$$\mathbf{\Theta}^T\dot{r} + \mathbf{Cv} = \mathbf{I} \quad (19)$$

where *M, C, K* and *Θ* are the mass, damping, stiffness and piezoelectric coupling matrices, respectively; *r* is the displacement vector; *m* is the mass distribution per unit length; M_t is the proof mass; w_b is the base excitation; *φ* is the vector of assumed mode shape which could be any admissible function; and *I* and *v* are the current and voltage vectors, respectively.

4. Mathematical modeling - Part II: aerodynamic model

In the above section, the electromechanical models are composed of the coupled mechanical equation and the circuit equation. The right hand side of the coupled mechanical equations is the forcing term due to base excitations. However, for aeroelastic piezoelectric energy harvesting, the forcing term corresponds to the aerodynamic force, usually at the free end, exerted by the incoming flow on the harvester. The mathematical model for the aerodynamic force depends on the specific aeroelastic instability phenomenon based on which the aeroelastic

energy harvester is designed to operate.

There have been many studies in the literature on the mathematical modeling of different types of aeroelastities, by researchers in both the area of aerodynamics and the area of small scale wind energy harvesting (Païdoussis *et al.* 2011, Hodges and Pierce 2002, Bryant and Garcia 2011, Williamson 1996, Sarpkaya 2004, Facchinetti *et al.* 2002, 2004, Barrero-Gil, Alonso *et al.* 2010, Barrero-Gil, Pindad *et al.* 2012, Sirohi and Mahadik 2011, 2012, Zhao, Tang *et al.* 2012, 2013, Zhao and Yang 2015a, b). This section presents the most classic aerodynamic modeling methods for each type of aeroelastic instability, which are most frequently employed to calculate the response of the aeroelastic energy harvesters.

4.1 Aerodynamic model for vortex-induced vibration

The complex aerodynamic force on the bluff body due to vortex shedding has been enthusiastically studied for many years. Early studies on VIV have mainly focused on 2D domain features, i.e., without considering the difference of elastic deformations along the cylinder's axial direction. In order to perform a preliminary evaluation on the attainable maximum power conversion efficiency of a VIV based harvester, Barrero-Gil, Pindado *et al.* (2012) presented a simplified mathematical model for a cylinder undergoing VIV, supported with a spring and damper. The equation of motion of the cylinder in the cross-flow direction is

$$m(\ddot{y} + 2\zeta\omega_n\dot{y} + \omega_n^2 y) = F_y(t) \quad (20)$$

where *m* is the mass per length; ζ is the damping ratio; ω_n is the fundamental frequency; F_y is the aerodynamic force per length exerted on the cylinder due to vortex shedding, expressed as

$$F_y(t) = \frac{1}{2}\rho_a U^2 DC_y(t) = \frac{1}{2}\rho_a U^2 DC_y\sin(2\pi ft + \varphi) \quad (21)$$

where ρ_a is the air density; *U* is the wind speed; *D* is the characteristic dimension (diameter here) of the cylinder; *f* is the oscillation frequency in Hz; φ is the phase difference between the aerodynamic force and the cylinder displacement; and C_y is the aerodynamic force coefficient. The steady state harmonic vibration can be depicted as

$$m(\ddot{y} + 2\zeta\omega_n\dot{y} + \omega_n^2 y) = F_y(t) \quad (22)$$

By substituting Eq. (21) into (20), the amplitude and oscillation frequency of vortex induced vibration were obtained and further normalized into dimensionless form as

$$A^* = \frac{C_y\sin\varphi}{16\pi^2 m^*\zeta}\left(\frac{U^{*2}}{f^*}\right) \quad (23)$$

$$f^* = \sqrt{1 - \frac{C_y\cos\varphi U^{*2}}{8\pi^2 m^* A^*}} \quad (24)$$

Employing the experimental measured results of the coefficients of $C_y\sin\varphi$ and $C_y\cos\varphi$ in the plane (A^*, V^*) $(V^*=U^*/f^*)$, Barrero-Gil, Pindado *et al.* (2012) iteratively calculated the normalized amplitude and frequency of VIV in Eqs. (23) and (24). For each fixed value of reduced wind speed V^*, A^* and f^* are increased by the respective step size, with $C_y\sin\varphi$ and $C_y\cos\varphi$ for a specific pair of (A^*, V^*) calculated by 2D spline interpolation. The process is finished until Eqs. (23) and (24) are satisfied within a prescribed tolerance.

Simplified one-dimensional model was also employed by Xie, Yang *et al.* (2012) to analyze the energy harvesting capability of a poled and electroded flexible ceramic cylinder under VIV. Besides these simplified models, the phenomenological models based on wake oscillators have been extensively used and modified to simulate the near wake vortex shedding dynamics (Balasubramanian, Skop *et al.* 2000, Facchinetti, De Langre *et al.* 2002). Besides simulating the 2D domain dynamics of VIV, wake oscillators have been frequently employed to study the 3D domain features of slender structures subject to VIV, such as tensioned cables, where the dynamics along the span wise direction has also been considered. Here we introduce the coupled models in the work of Facchinetti, De Langre *et al.* (2004). A nonlinear wake oscillator described in a van der Pol equation is coupled with the structure oscillator, which describes the equation of motion of the bluff body. This wake oscillator-based model has been employed to predict the power response of a VIV harvester (Dai, Abdelkefi *et al.* 2014a, b) and verify the effectiveness of the proposed strategy of enhancing the power output with a beam stiffener (Zhao and Yang 2015a).

The structure oscillator is given by

$$\left(m+m_f\right)\left(\ddot{y}+2\zeta\omega_n\dot{y}+\frac{r_f}{m+m_f}\dot{y}+\omega_n^2 y\right)=S \qquad (25)$$

Besides the parameters that have already been described in Eq. (20), m_f and r_f are the distributed fluid-added mass and damping, respectively, expressed as

$$m_f=\frac{C_M\rho D^2\pi}{4} \qquad (26)$$

$$r_f=\frac{C_D}{4\pi St}\omega_f\rho D^2 \qquad (27)$$

where C_M is the fluid added mass coefficient and set as $C_M=1$ for a circular cross section; C_D is the mean sectional drag coefficient and set as $C_D=2.0$ in the range of Re: $300<Re<1.5\times10^5$. S is the vortex shedding induced alternating force which is coupled with the wake oscillator. The nonlinear wake oscillator is described in the van der Pol equation

$$\ddot{q}+\varepsilon\omega_f\left[q^2-1\right]\dot{q}+\omega_f^2 q=F \qquad (28)$$

where q is a dimensionless wake variable, ε is a constant van der Pol parameter, and F is the forcing term of the wake oscillator. The structure-fluid coupling terms, S and F, are

related to q and acceleration, as

$$S=\frac{1}{4}\rho DU^2 C_{L0}q, \quad F=\frac{A}{D}\ddot{y} \qquad (29)$$

where C_{L0} is the reference lift coefficient on a fixed cylinder undergoing vortex shedding, set as $C_{L0}=0.3$ in the range of $300<Re<1.5\times10^5$; and A is a constant scaling parameter of the F. It should be mentioned that according to Facchinetti, De Langre *et al.* (2004), there exist other two coupling forms besides the acceleration coupling introduced here, which are, respectively, the displacement coupling $F=(A/D)y$, and the velocity coupling $F=(A/D)\dot{y}$. The mentioned constant parameters, ε and A, can be obtained from experiments and are suggested being taken as $\varepsilon=0.3$ and $A=12$ for all the above three coupling methods (Facchinetti, De Langre *et al.* 2004).

4.2 Aerodynamic model for galloping

Consider a bluff body undergoing galloping shown in Fig. 5(a). The aerodynamic model for galloping is based on the quasi-static hypothesis (Den Hartog 1956, Païdoussis, Price *et al.* 2011), which is applicable to most cases of galloping since the characteristic timescale of flow (U/h) is small compared to the characteristic timescale of oscillation ($2\pi/\omega_n$). Mathematical modeling of the aerodynamic force due to galloping is given by

$$F_{tip}=\frac{1}{2}\rho_a hlU^2 C_{Fz} \qquad (30)$$

where h is the frontal dimension facing the wind flow; l is the length of the tip body; and C_{Fz} is the total aerodynamic force coefficient. It is convenient to express C_{Fz} with a polynomial expansion, which is usually obtained by fitting to the experimental results, given by (Païdoussis, Price *et al.* 2011)

$$C_{Fz}=\sum_i A_r(\frac{\dot{w}}{U})^r, r=1,2,3,... \qquad (31)$$

where A_r is the empirical coefficient for the polynomial fitting. For numerical values of A_r for several cross section shapes in smooth flow, readers are referred to Païdoussis, Price *et al.* (2011) after the work of Novak (1969) and Novak and Tanaka (1974).

It should be noted that turbulence in the flow varies the values of A_r. Take the D-section for instance, referring to the galloping criterion in Eq. (6), $A_1=\partial C_{Fz}/\partial\alpha=-0.097431<0$ in smooth flow, so the D-section is not able to reach "self-excited" galloping, but an external large perturbation is necessary. However, if the flow condition is changed to be with 11% turbulence density, A_1 becomes $0.79>0$ for the D-section (Barrero-Gil, Alonso *et al.* 2010), which enables it to undergo self excited galloping. Moreover, the degree of the expansion polynomial of C_{Fz} affects the response of galloping (Sorribes-Palmer and Sanz-Andres 2013). For example, if a fifth or seventh-order polynomial representation of C_{Fz} for a square section is used, the predicted response of vibration amplitude versus

wind speed shows a hysteresis phenomenon in a specific portion, as shown in Fig. 6(b). However, if a third-order polynomial is used, the hysteresis region disappears, with the response similar to that in Fig. 6(a). We have determined that a third-order polynomial predicts acceptable responses since the hysteresis phenomenon is hard to observe in the experiment of galloping-based harvester (Zhao, Tang *et al.* 2013, Yang, Zhao *et al.* 2013). Cubic polynomial C_{Fz} expressions have also been employed by Dai, Abdelkefi *et al.* (2015) for the theoretical analysis of a electromagnetic energy harvester and by Bibo and Daqaq (2014) and Bibo, Alhadidi *et al.* (2015), Bibo, Abdelkefi *et al.* (2015) for piezoelectric energy harvesters with well agreed predicted results with those from experiments.

Besides using the expansion polynomial of C_{Fz} to calculate the galloping force, another method is to perform a table lookup to find the corresponding values of lift or drag coefficients at a specific angle of attack directly from the measured data. Sirohi and Mahadik (2011, 2012) employed this table lookup method to calculate the galloping forces on a triangular section and a D-section for the purpose of wind energy harvesting.

4.3 Aerodynamic model for flutter

As mentioned in Section 2.3, among the frequently studied three forms of flutter, i.e., cross flow flutter of plates or belts, axial flow flutter of cantilevered plates, and modal convergence flutter of airfoils, the airfoil flutter has attracted the most interests for energy harvesting. In this section, we introduce the theoretical modeling methods that are suitable for predicting the power response of an energy harvester based on the aeroelastic flutter of an airfoil. The aerodynamic models are classified into two main categories: the linear aerodynamic model and the nonlinear aerodynamic model. The former is often exploited to conduct the flutter boundary analysis, while the latter is required to analyze the limit cycle oscillations beyond the flutter boundary. The power output from an airfoil flutter based energy harvester can be readily calculated by incorporating the aforementioned electromechanical model with one of the following aerodynamic models.

4.3.1 Linear aerodynamics
Steady flow theory
As shown in Fig. 8(a), a typical airfoil section subjected to wind flows is elastically mounted using a compression-extension spring and a torsion spring. The four points of Q, C, P and T represent, respectively, the quarter-chord which is assumed to be the aerodynamic center, the center of mass, the reference point where the plunge displacement is measured, and the three-quarter-chord (Hodges and Pierce 2002). The equations of motion of the airfoil section are given by

$$m\ddot{h} + mbx_\theta\ddot{\theta} + d_h\dot{h} + k_h h = -L \qquad (32)$$

$$I_P\ddot{\theta} + mbx_\theta\ddot{h} + d_\theta\dot{\theta} + k_\theta\theta = M_{\frac{1}{4}} + b(\frac{1}{2} + a)L \qquad (33)$$

where h and θ are the plunge displacement and pitch displacement, respectively; m is the mass per length in the span direction; b is the semichord length; I_P is the moment of inertia per length about the reference point; d_h and d_θ are the damping per length in the plunge and pitch degrees of freedom, respectively; k_h and k_θ are the stiffness per length in the plunge and pitch degrees of freedom, respectively; a is the dimensionless parameter that is used to determine the location of the reference point from the leading edge; and x_θ is the dimensionless chordwise offset of the center of mass from the reference point, denoted by $x_\theta = e-a$, with e determining the location of the center of mass. L and $M_{1/4}$ are the aerodynamic lift per length and the aerodynamic pitching moment per length about the quarter-chord, respectively. With the steady flow theory, they are calculated by

$$L = \frac{1}{2}\rho_a\left(2b\right)U^2 C_L = 2\pi\rho_a bU^2\theta \qquad (34)$$

$$M_{\frac{1}{4}} = 0 \qquad (35)$$

where C_L is the effective lift coefficient, which is taken to be $C_L = 2\pi\theta$ when steady flow theory for a thin airfoil is employed. The angle of attack is simply taken as the instantaneous pitch angle θ. The lift-curve slope is taken to be 2π.

Unsteady flow theory
The steady flow theory comes in a quite simple form. However, it has unacceptable deficiency in predicting the flutter boundary and modal frequencies at the boundary. Unsteady aerodynamic effects are important due to at least the following three facts, as summarized by Hodges and Pierce (2002). First, the direction of relative wind vector is not fixed in space due to the airfoil's oscillatory motion, changing the effective angle of attack; second, vortex shedding at the trailing edge is induced by the airfoil's oscillation, the downwash from which also changes the effective angle of attack; third, the apparent mass and inertia effects should be considered because the air particles surrounding the airfoil are accelerated by its oscillatory motion. In an unsteady flow model, both circulatory and noncirculatory terms should be included. In the literature, the most commonly studied unsteady flow theories include the Theodorsen's unsteady thin-airfoil theory (Theodorsen 1934) and the finite-state unsteady thin-airfoil theory of Peters, Karunamoorthy *et al.* (1995).

(1) Theodorsen's unsteady thin-airfoil theory
The unsteady flow theory derived by Theodorsen (1934) assumes that the airfoil undergoes small amplitude harmonic oscillations in incompressible flow. This theory has been frequently employed in predicting the power output responses of airfoil flutter based energy harvesters at the flutter boundary (Erturk *et al.* 2010, Sousa, De M

Anicézio *et al*. 2011, De Marqui and Erturk 2012). The aerodynamic lift includes both circulatory and noncirculatory terms, while the aerodynamic pitching moment about the quarter-chord includes noncirculatory term only. The expressions are given by

$$L = 2\pi\rho_a bUC(k)\left[\dot{h}+U\theta+b\left(\frac{1}{2}-a\right)\dot{\theta}\right]+\pi\rho_a b^2\left(\ddot{h}+U\dot{\theta}-ba\ddot{\theta}\right) \quad (36)$$

$$M_{\frac{1}{4}} = -\pi\rho_a b^3\left[\frac{1}{2}\ddot{h}+U\dot{\theta}+b\left(\frac{1}{8}-\frac{a}{2}\right)\ddot{\theta}\right] \quad (37)$$

The first term in Eq. (36) accounts for the circulatory effect, while the second term in Eq. (36) and the term in Eq. (47) account for the noncirculatory effects. The circulatory lift is the most significant among all these terms. Comparing Eq. (36) with Eq. (34), it can be inferred that an effective angle of attack is introduced, given by

$$\alpha = C(k)\left[\theta+\frac{\dot{h}}{U}+\frac{b}{U}\left(\frac{1}{2}-a\right)\dot{\theta}\right] \quad (38)$$

This effective angle of attack is calculated at the three-quarter chord, point T in Fig. 8(a), and takes in account the induced flow over the chord. The lift-deficiency function $C(k)$ is a complex-valued function of the reduced frequency $k=b\omega/U$ with ω being the frequency of motion. The involvement of $C(k)$ decreases the magnitude of the unsteady lift when compared to the value obtained directly from the steady flow theory, and introduces a phase difference between the plunge and pitch motions.

It is worth noting that the quasi-steady linear flow model, which is obtained by taking $C(k)$ to be unity in Eq. (36), is a simplified and commonly used model to approximately predict the time dependent responses of the airfoil at the flutter boundary. The airfoil is assumed to have the same aerodynamic characteristics as the one moving with constant pitching and plunging velocity equal to the instantaneous values (Fung 1955). This is only acceptable for the situations where the characteristic timescale of flow is small compared to the characteristic timescale of oscillation as clarified in the galloping model.

(2) Finite-state unsteady thin-airfoil theory of Peters, Karunamoorthy *et al*. (1995)

Unlike the Theodorsen's theory, the finite-state theory of Peters, Karunamoorthy *et al*. (1995) does not assume simple harmonic oscillations. As a time-domain model with state-space form representation, it is capable of calculating eigenvalues below the flutter speed and applicable in designs for active control of flutter. It has also been employed in the study of flutter energy harvesting at the flutter boundary (Bryant and Garcia 2009, 2011). The accuracy and validity of this model have been confirmed by the wind tunnel test of their harvester prototype. The circulatory effects of vortex shedding are approximated by introducing an induced-flow term, i.e., the average induced-flow velocity λ_0, which is further represented with a set of time-domain differential equations. The lift and pitching moment are expressed as

$$L = 2\pi\rho_a bU\left[\dot{h}+U\theta+b\left(\frac{1}{2}-a\right)\dot{\theta}-\lambda_0\right]+\pi\rho_a b^2\left(\ddot{h}+U\dot{\theta}-ba\ddot{\theta}\right) \quad (39)$$

$$M_{\frac{1}{4}} = -\pi\rho_a b^3\left[\frac{1}{2}\ddot{h}+U\dot{\theta}+b\left(\frac{1}{8}-\frac{a}{2}\right)\ddot{\theta}\right] \quad (40)$$

It can be noted that the expression of the pitching moment is the same with that in the Theodorsen's theory. λ_0 is represented in terms of N induced-flow states λ_n as

$$\lambda_0 \approx \frac{1}{2}\sum_{n=1}^{N}b_n\lambda_n \quad (41)$$

where λ_n can be obtained from a set of N differential equations given by

$$[A]\{\dot{\lambda}\}+\frac{U}{b}\{\lambda\} = \{c\}\left[\ddot{h}+U\dot{\theta}+b\left(\frac{1}{2}-a\right)\ddot{\theta}\right] \quad (42)$$

The expressions of the related matrices are given as follows

$$[A] = [D]+\{d\}\{e\}^T+\{c\}\{d\}^T+\frac{1}{2}\{c\}\{e\}^T \quad (43)$$

$$D_{nm} = \begin{cases} \dfrac{1}{2n} & n=m+1 \\[2mm] -\dfrac{1}{2n} & n=m-1 \\[2mm] 0 & n\neq m\pm 1 \end{cases} \quad (44)$$

$$e_n = \begin{cases} (-1)^{n-1}\dfrac{(N+n-1)!}{(N-n-1)!}\dfrac{1}{(n!)^2} & n\neq N \\[3mm] (-1)^{n-1} & n=N \end{cases} \quad (45)$$

$$d_n = \begin{cases} \dfrac{1}{2} & n=1 \\[2mm] 0 & n\neq 1 \end{cases} \quad (46)$$

$$c_n = \frac{2}{n} \quad (47)$$

4.3.2 Nonlinear aerodynamics

Although the aforementioned sophisticated aerodynamic models like those of Theodorsen and Peters et al are adequate to predict aeroelastic and power output responses of flutter based harvesters near the flutter boundary, they are

both based on linear assumptions, where the angle of attack is regarded to remain small, i.e., below the critical angle of attack to induce stall, and the attached flow over the airfoil is dominant. With this assumption, the amplitude of oscillation grows exponentially at a wind speed above the flutter speed. Theoretical modeling of flutter energy harvesters with the Theodorsen's or finite-state linear theory is merely able to predict the power response just above the flutter speed. To accurately study the aeroelastic as well as power output responses of a harvester undergoing limit cycle oscillations far away from the flutter boundary, nonlinearity has to be introduced into the model. Either structural nonlinearity (i.e., material nonlinearity and geometry nonlinearity) or aerodynamic nonlinearity can induce limit cycle oscillations above the flutter boundary. Structural nonlinearities can be due to large displacement of wings, loose linkages and worn hinges, and nonlinearities in stiffness properties of other components. Classical types of stiffness nonlinearities like the cubic nonlinearity, hysteresis nonlinearity and freeplay nonlinearity have drawn wide attentions in the research of aeroelasticity in aircraft (Zhao and Yang 1990, Dugundji 1992, Lee, Price *et al*. 1999, Dowell, Edwards *et al*. 2003, Abdelkefi and Hajj, 2013, Xiang, Yan *et al*. 2014). Inspired from this, in flutter based energy harvesting, some researchers considered the stiffness nonlinearity in the analysis of power responses (Sousa, De M Anicézio *et al*. 2011, Abdelkefi, Nayfeh *et al*. 2012b, c, d). On the other hand, the aerodynamic nonlinearities arise from the stalling phenomenon, where the separated airflow over the wing becomes dominant, and the aerodynamic lift force begins to decrease (Fung 1955, Balakrishnan 2012, Dowell 2015). The critical angle of attack where flutter stall occurs is typically in the range of 8 to 20 degrees. The flap rotation of the airfoil for a flutter based energy harvester is most likely to surpass this critical value (Bryant and Garcia 2011), making the nonlinear aerodynamic modeling necessary for accurate power output prediction. Next, we introduce typical nonlinear aerodynamic modeling methods in the literature.

Quasi steady model based on the effective angle of attack

The quasi-steady nonlinear aerodynamic model is based on the concept of effective angle of attack (Fung 1955, Strganac, Ko *et al*. 2000) in the aforementioned Theodorsen's linear model. Extra nonlinear terms are simply introduced to it to approximate the aerodynamic lift at large angles of attack. As a common practice, noncirculatory terms are further ignored in this model. The expressions of the lift and moment are given by

$$L = 2\pi\rho_a bU^2 \left\{ \left[\theta + \frac{\dot{h}}{U} + \frac{b}{U}\left(\frac{1}{2}-a\right)\dot{\theta} \right] - c_s \left[\theta + \frac{\dot{h}}{U} + \frac{b}{U}\left(\frac{1}{2}-a\right)\dot{\theta} \right]^3 \right\} \quad (48)$$

$$M_{\frac{1}{4}} = 0 \quad (49)$$

where c_s is a nonlinear parameter related to the flutter stall and can be determined from the measured lift curve in the wind tunnel experiment. As in the case of linear aerodynamics, the quasi-steady model is only applicable for slow harmonic oscillations with low frequency in subsonic flow, e.g., for a harvester that is designed to own relatively low natural frequencies, say, smaller than 10Hz. This model has been employed in flutter based energy harvesting by Abdelkefi, Nayfeh *et al*. (2012a, b, c) and Bibo and Daqaq (2013a, b).

Semi-empirical unsteady nonlinear aerodynamic model based on ordinary differential equations

One commonly exploited semi-empirical unsteady nonlinear aerodynamic model is the ONERA model, which was initially developed by Tran and Petot (1981) and Dat and Tran (1983). Modification was made later by Peters (1985) on the effective angle of attack. This model has been applied to extensive studies on the nonlinear characteristics of airfoil flutter (Mcalister, Lambert *et al*. 1984, Dunn and Dugundji 1992, Chen 1993, Tang and Dowell 1996). In this model, the aerodynamic lift on an airfoil subjected to flutter stall is associated with the angle of attack in the form of an ordinary differential equation. Coefficients are determined from the experimental data. The static force curve of the airfoil is employed, with a single lag term introduced to the linear portion where the Theodorsen's linear theory is used, and two lag terms introduced to the stall portion (Chen 1993).

The ONERA model was first introduced into the study of flutter based energy harvesters by Bryant and Garcia (2011), with very well agreed predictions with experiments achieved for the flutter response and power outputs. The model is described as follows.

$$C_z = C_{z1} + C_{z2} \quad (50)$$

$$C_{z1} = s_{z1}\dot{\alpha} + s_{z2}\ddot{\theta} + s_{z3}\dot{\theta} + C_{z\gamma} \quad (51)$$

$$\dot{C}_{z\gamma} + \lambda_1 C_{z\gamma} = \lambda_1 a_{0L}\left(\alpha+\dot{\theta}\right) + \lambda_2 a_{0L}\left(\dot{\alpha}+\ddot{\theta}\right) \quad (52)$$

$$\ddot{C}_{z2} + r_1\dot{C}_{z2} + r_2 C_{z2} = -r_2\Delta C_z\big|_\alpha - r_3\Delta\dot{C}_z\big|_\alpha \quad (53)$$

Note that the dot is the derivative with respect to the dimensionless time $\tau=Ut/b$. In the above equations, C_z stands for any relative aerodynamic force coefficient, i.e., C_L for lift, C_D for drag or C_M for moment. C_{z1} represents the contribution of the linear force, which further includes the circulatory terms ($C_{z\gamma}$) and the noncirculatory terms; while C_{z2} represents the contribution of the nonlinear force, which has to be considered when the static force curve deviates from the extension of the linear portion, as shown in Fig. 12. In general, a_{0L} is taken as 2π as the lift-curve slope in the linear portion. The parameters s_{z1}, s_{z2}, s_{z3}, λ_1, λ_2, r_1, r_2, and r_3 are empirically derived by fitting to results of wind tunnel experiment, of which the identification process has been discussed a lot in the literature (Mcalister, Lambert *et al*. 1984, Dunn and Dugundji 1992, Chen 1993).
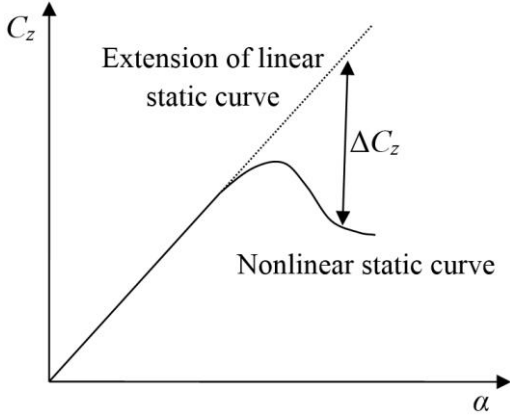
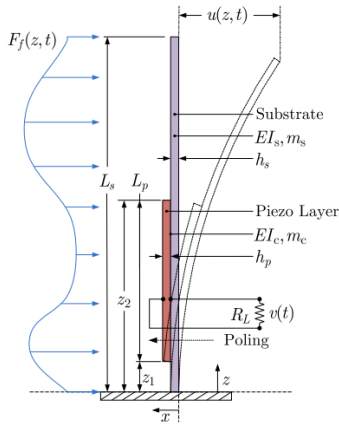Fig. 12 Concept of ONERA unsteady nonlinear aerodynamic model

Fig. 13 Schematic of cantilevered unimorph harvester for statistical model of turbulence-induced force (Hobeck and Inman 2014)

Besides the ONERA model, there are other semi-empirical models that have yet been but are potential to be employed for power output predictions of flutter based energy harvesters, e.g., the one proposed by Mahajan, Kaza *et al*. (1993) which assumes that the aerodynamic forces behave like a damped harmonic oscillator. Recently, a low-order quasi-steady model based on rotational lift and a revised version incorporating dynamic stall was proposed by Gomez, Bryant *et al*. (2014). This model was experimentally validated with the scale and shape of the force curves similar to the experimental data, providing an alternate method for modal convergence flutter based energy harvesting.

4.4 Aerodynamic model for wake galloping

As mentioned in Section 2.4, due to the complexity of upstream wakes, the characteristics of wake galloping (Tokoro, Komatsu *et al*. 2000) and the performance of wake galloping based energy harvesters (Jung and Lee 2011, Hobbs and Hu 2012, Abdelkefi, Scalon *et al*. 2013) were basically evaluated via experiments. The measured results of Jung and Lee (2011) showed that obvious displacement occurred for configurations with *L*=3*D* to *L*=6*D*, which can serve as a rough guidance for proper arrangement of the twin cylinders. Tokoro, Komatsu *et al*. (2000) conducted an

experimental study on the wake galloping of twin cables and investigated the influence of various parameters on the aerodynamic characteristics including the spacing, Reynolds number, incidence angle of the wind, damping and natural frequency of the system. It was found that the maximum amplitude of vibration occurs at *L/D*=4.3 with an incidence angle of the wind of 15°. Also, the vibration direction is not exactly normal to the wind flow, but inclined to it with a small angle. For detailed results readers are referred to the work of Tokoro, Komatsu *et al*. (2000).

As for wake-induced flutter, theoretical models do exist in various forms, including the linear model that predicts the instability boundary as well as the nonlinear model that calculates the amplitude of limit cycle oscillation (Païdoussis, Price *et al*. 2011). There is an interesting finding that an increase in structural damping does not necessarily reduce the amplitude of oscillation of the leeward cylinder, whereas it increases the extraction of the flow energy. Future designs of energy harvesters based on wake-induced flutter should take this point into account. For a detailed analysis of the characteristics of wake-induced flutter, readers are referred to the review work of Païdoussis, Price *et al*. (2011).

4.5 Aerodynamic model for turbulence-induced vibration

Theoretical modeling of turbulence-induced force is not as straightforward as that of the aforementioned types of aerodynamic forces, due to the random noises in the turbulent flow. Mean velocity and turbulence density are not sufficient to fully represent the characteristics of the flow, not to mention the characteristics of the induced force. In order to conduct a theoretical analysis of their previous prototypes of piezoelectric grass-typed harvester (Hobeck and Inman 2012b) mentioned in Section 2.5, Hobeck and Inman (2014) proposed a statistical model to simulate the distributed turbulence-induced force along a unimorph cantilever. This model requires time-series dynamic pressure measurements from the experiment, which are accomplished using dual pressure probes. Details of the design and analysis of the pressure probes were included in another work of Hobeck and Inman (2012a). Being verified with wind tunnel experiments, the displacement and power responses of their prototype were successfully predicted with this statistically derived aerodynamic model. Here we introduce the basic procedure of this model. For more detailed derivation process, readers are referred to the paper of Hobeck and Inman (2014).

Fig. 13 shows the schematic of cantilevered unimorph harvester for the derivation of statistical model. The model is based on the acceptance integral approach proposed by Powell (1958). The acceptance integral is given by

$$J_{mn}(\omega) = \int_0^{L_s} \int_0^{L_s} \phi_m(z) S_p(z, z', \omega) \phi_n(z') dz dz' \quad (54)$$

where *J* is the acceptance; L_s is the length of the cantilever; ϕ is the mode shape; *z* and *z'* denote the vertical locations of the measured points along the cantilever; ω is the frequency of oscillation; S_p is the pressure cross-power spectral

density (CPSD) which is obtained from experimental measurements using the pressure probes, with its expression given by

$$S_p(z,z',\omega) = \lim_{T\to\infty} \frac{1}{4\pi T} \int_{-\infty}^{\infty} \left\{ \int_{-T}^{T} E\big[p(z,t)p(z',t+\tau) \big] dt \right\} e^{-j\omega t} d\tau \quad (55)$$

where p is the measured pressure; E is an expectation of the two pressure signals that must be taken; and T and τ are the sample time and time offset, respectively. With the experimental measurements, the statistically obtained modal distributed turbulence-induced forcing term is given by

$$\overline{\psi}_m(t) = \left(H_m^{-1} \sqrt{2A\int_{-\omega_s}^{\omega_s} |H_m|^2 J_{mm} d\omega} \right) e^{j\omega t} \quad (56)$$

where H_m is the modal displacement frequency response function expressed as

$$H_m = \frac{1}{(m_m + \mu_m)(\omega_m^2 - \omega^2 + 2j\zeta_m\omega_m\omega)} \quad (57)$$

with m_m, μ_m and ζ_m being the modal beam mass, fluid added mass and modal damping, respectively. Because measured data from experiments are essential, the accuracy of this model significantly depends on the electrical noise and bandwidth limitations of the pressure probes (Hobeck and Inman 2012a).

5. Equivalent circuit modeling

Using the mathematical models incorporating the electromechanical model and the aerodynamic model, the electromechanical and fluid-structure coupling behaviors can be readily analyzed when the interface circuit is kept simple, i.e., a pure resister for power dissipation. However, for practical applications in WSN nodes and other electronics, the interface circuit connected to an energy harvester will be more complex for the process of AC-DC signal rectification and regulation, or for further storage of energy (Lallart and Guyomar 2008, Wickenheiser, Reissman *et al.* 2010, Liang and Liao 2012, Lien, Shu *et al.* 2010, Lefeuvre, Badel *et al.* 2006, 2007, Li, Xiang *et al.* 2013). In such a case, theoretical formulations for the harvesting process become much complicated due to the added nonlinear electronic components in the circuit. To solve this problem, researchers have proposed equivalent circuit models for vibration piezoelectric and electromagnetic energy harvesters (Elvin and Elvin 2009a, b, Yang and Tang 2009).

The equivalent circuit model is established based on the analogies between the relationships of parameters in the mechanical and electrical domains. For example, $F = M\ddot{x}$, $F = C\dot{x}$ and $F = Kx$ in the mechanical domain is analogous in the form to $V = L\ddot{q}$, $V = R\dot{q}$ and $V = (1/C_0)q$, respectively, with F, M, C, K and x representing the mechanical force, mass, damping and stiffness, respectively, and V, L, R, C_0 and q representing the voltage, inductance, load resistance, capacitance and

electrical charge, respectively. The earliest uncoupled equivalent circuit model simulated the piezoelectric energy harvester with an ideal current source in parallel with its internal capacitance, or with an ideal voltage source in series with its internal capacitance. Elvin and Elvin (2009a) proposed an equivalent circuit model for vibration energy harvester in which the electromechanical coupling was taken into account. The derivation process was based on the Rayleigh-Ritz model with a series of assumed displacement modes. Later, a coupled finite element–circuit simulation model was proposed by Elvin and Elvin (2009b), which is capable of analyzing complicated mechanical structures and electrical circuits utilizing the powerful tools of finite element analysis (FEA) like ANSYS or ABAQUS and electrical simulators like SPICE. The two parts of simulations were conducted separately, and post-processing of data extraction and transfer was required for the coupling between the two parts. Yang and Tang (2009) proposed an equivalent circuit model where the system parameters can be efficiently obtained from theoretical analysis or FEA. Example studies of energy harvester with both simple and complicated geometries were conducted. The schematic of the multi-mode equivalent circuit model for a vibration energy harvester is shown in Fig. 14 (Yang and Tang 2009).

As for aeroelastic energy harvesters, a new problem arises since the external aerodynamic forces are displacement-dependent nonlinear forces, unlike in vibration energy harvesting, where the base excitation force is independent of the system displacement and can be easily simulated with a separate voltage source component in the equivalent circuit model (see V_1, $V_2…V_r$ in Fig. 14). To solve this problem, Tang, Zhao *et al.* (2015) proposed an equivalent circuit representation method for galloping-based piezoelectric energy harvesters, representing the nonlinear aerodynamic force with a user-defined electronic component with a nonlinear transfer function, as shown in Fig. 15. The meanings of the symbols in the equivalent circuit model are given in Table 1. The aerodynamic force was represented with a voltage source given by

$$V(t) = -\frac{1}{2}\rho_a h l U^2 \sum_{i=1,2…} A_i \left[\frac{\dot{q}(t)}{U} + \beta C V_C(t) \right]^i \quad (58)$$

where the term in the bracket indicated the modified angle of attack taking into account the beam rotation at the free end, i.e., modifying Eq. (4) into $\alpha = \dfrac{\dot{w}}{U} + \beta w$ with β being an angle coefficient. The voltage V_C across the capacitor C was employed to calculate the charge q with $q = C V_C$. The proposed model was validated with wind tunnel experimental results.

Elvin (2014) proposed two approaches, i.e., a system-level approach and a dependent source equivalent approach, to model the behaviors of advanced energy harvesters with nonlinear component, e.g., a vibration energy harvester with nonlinear stiffness (Duffing harvester), or aeroelastic energy harvester with nonlinear aerodynamic force. For a 2DOF flutter-based energy harvester, of which the aerodynamic mechanism has been introduced in Sections 2.2.1.3 and 2.2.3.3, the equivalent circuit model is shown in Fig. 16.
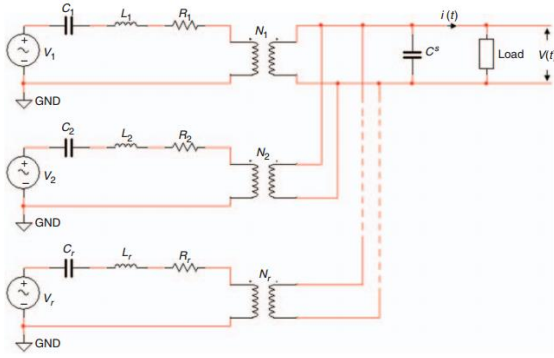
Fig. 14 Schematic of multi-mode equivalent circuit model for a vibration energy harvester (Yang and Tang 2009)

Table1Analogy between mechanical and electrical domain, adapted from Tang, Zhao *et al.* (2015)

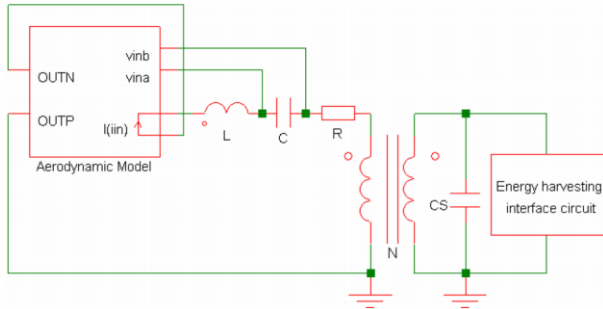| Equivalent electrical parameters	Mechanical parameters
Charge $q(t)$	Displacement $w(t)$
Current $\dot{q}(t)$	Velocity $\dot{w}(t)$
Inductance L	Effective mass M
Resistance R	Effective damping D
Capacitance C	Reciprocal of effective stiffness $1/K$
Transformer turn ratio N	Electromechanical coupling Θ

Fig. 15 Schematic of equivalent circuit representation for a galloping-based piezoelectric energy harvester (Tang, Zhao *et al.* 2015)

The governing equation of the harvester was expressed similar to Eqs. (32) and (33), with

$$m\ddot{x} + D\dot{x} + Kx - \Theta V + \left(me\ddot{\alpha} - H_1\dot{x} - H_3\alpha\right) = F(t)$$
$$I_\alpha\ddot{\alpha} + D_\alpha\dot{\alpha} + K_\alpha\alpha + \left(me\ddot{x} - A_1\dot{x} - A_3\alpha\right) = M(t) \tag{59}$$

where x, α, V, m, I_α, D, D_α, K, K_α, e and Θ were the plunge displacement, pitch displacement, generated voltage in the piezoelectric element, airfoil mass, airfoil moment of inertia, plunge damping, pitch damping, plunge stiffness, pitch stiffness, offset of the center of mass from the reference point and electromechanical coupling, respectively; $F(t)$ and $M(t)$ were indicated as the aerodynamic lift and moment, of which the formulations were not specified; and H_1, H_3, A_1 and A_3 were the aerodynamic force coefficients. With such a governing equation, the equivalent circuit model was established by adding the two nonlinear terms in the parentheses at the left side as two voltage-dependent sources NV_1 and NV_2. During circuit simulation, they were defined with the voltage across the standard circuit components by

$$NV_1 = \frac{V(I_\alpha)}{I_\alpha}me - H_1\frac{V(D)}{D} - H_3\frac{V\left(\frac{1}{K_\alpha}\right)}{K_\alpha}$$
$$NV_2 = \frac{V(m)}{m}me - A_1\frac{V(D)}{D} - A_3\frac{V\left(\frac{1}{K_\alpha}\right)}{K_\alpha} \tag{60}$$

Although the validation process of the proposed equivalent circuit model for the flutter harvester was not provided, a similar equivalent circuit model for a nonlinear electromagnetic Duffing harvester was validated theoretically, verifying the proposed voltage-dependent source equivalent approach.

A great advantage of the equivalent circuit model is that it enables the practical interface circuit with nonlinear power extraction process to be taken into account. The complex coupling behaviors between the mechanical structure, piezoelectric transducer, aerodynamic force, and the complex interface circuit are evaluated simultaneously via system-level circuit simulation. With the benefit of the equivalent circuit model, Zhao, Tang *et al.* (2014b, 2016) investigated the performance enhancing feasibility of a self-powered synchronized charge extraction (SCE) interface in a galloping piezoelectric energy harvester system. System-level simulation was conducted integrating the equivalent circuit model and the SCE diagram as shown in Fig. 17, which revealed three main advantages of SCE in galloping harvesters: eliminating the requirement of impedance matching, saving 75% of piezoelectric material and alleviating fatigue with reduced mechanical displacement. System-level simulation based on the equivalent circuit model was also conducted by Zhao and coworkers (Zhao, Liang *et al.* 2015) to investigate the power enhancing capability of a self-powered synchronized switching harvesting on inductor interface in a galloping piezoelectric energy harvester system.

However, it has to be noted that, if the mechanical structure of the harvester is complex, e.g., with odd shaped cantilevers, additional efforts in finite element analysis (FEA) are required to identify the analogical circuit parameters.
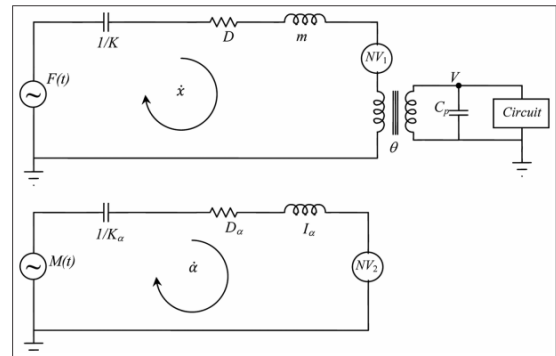

Fig. 16 Schematic of equivalent circuit model for a 2DOF flutter-based piezoelectric energy harvester (Elvin 2014)
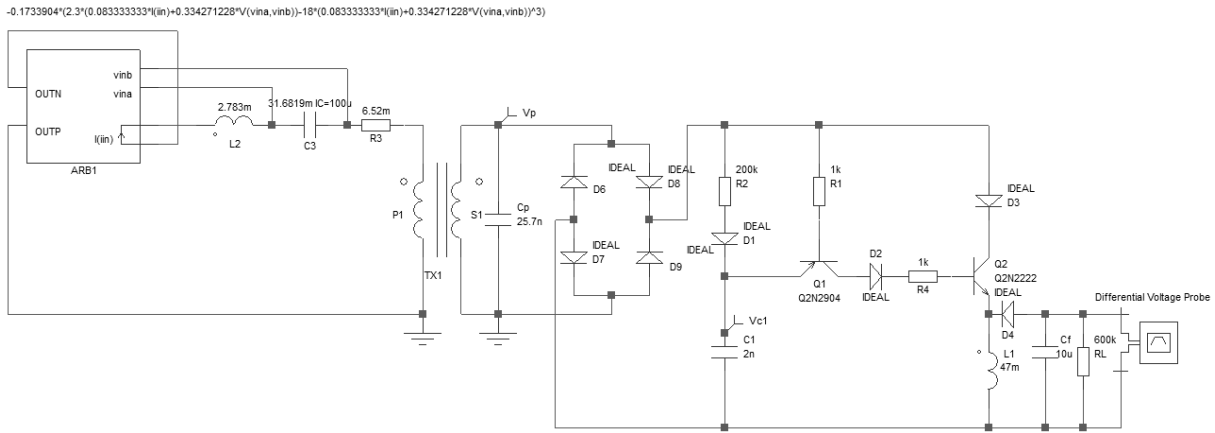
-0.1733904*(2.3*(0.083333333*I(iin)+0.334271228*V(vina,vinb))-18*(0.083333333*I(iin)+0.334271228*V(vina,vinb))^3)

Fig. 17 Equivalent circuit model diagram integrating a self-powered SCE circuit with a galloping piezoelectric energy harvester (Zhao, Tang *et al*. 2016)
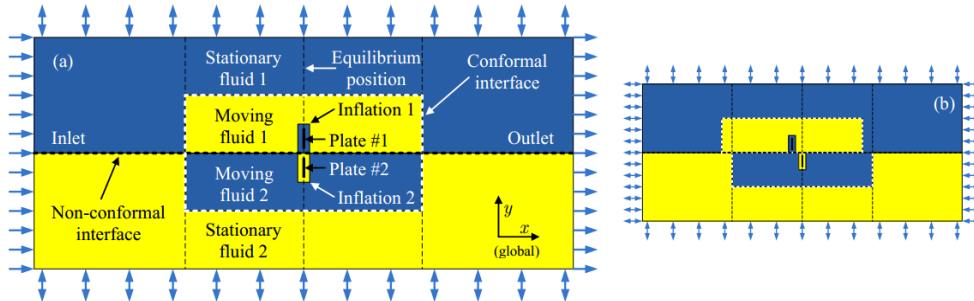
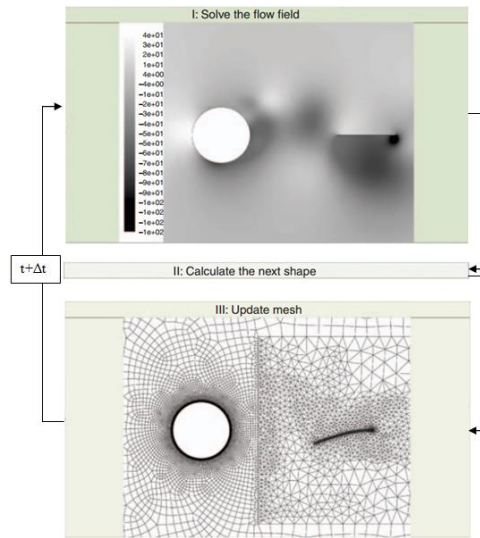Fig. 18 Computational domain and meshing zones in CFD model for DCF harvester (Hobeck, Geslain *et al*. 2014)

Fig. 19 Procedure and meshing details for CFD simulation (Akaydin, Nayfeh *et al*. 2010a)

6. Modeling based on computation fluid dynamics (CFD)

Besides the mathematical and equivalent circuit modeling, some researchers have employed computational fluid dynamics (CFD) to simulate the complex interactions between the fluid flow and the solid structure of the energy harvester, utilizing the commercial CFD simulation software like the COMSOL Multiphysics, ANSYS-CFX, ANSYS-FLUENT, etc. It is beyond the scope of this review paper to present and compare the detailed coding and meshing process of various CFD modeling methods, interested readers are referred to the respective software manuals and related technical literatures (COMSOL CFD Module, ANSYS CFX, ANSYS Fluent, Computational fluid dynamics, Wikipedia). Here we introduce the recent flow

energy harvesting studies with applications of CFD.

Sivadas and Wickenheiser (2011) conducted a parametric study on a VIV based piezoelectric energy harvester, which consisted of an upstream fixed bluff body and a piezoelectric cantilever attached to its trailing edge. CFD simulations with the COMSOL Multiphysics software were run for different dimensions and shapes of the bluff body, length and thickness of the beam and Reynolds number to investigate their effects on the lock-in bandwidth and output power. It was found that a medium long beam with a length-to-diameter ratio of 2 to 2.5 could induce the maximum strain on the beam because it enabled the vortex streets to form at the right position to excite the beam's fundamental mode. Among the three considered bluff body shapes, i.e., cylinder, triangle and pentagon, it was shown that the triangular bluff body had a narrow lock-in bandwidth at a low Reynolds number region, while the cylindrical and pentagonal bluff bodies had wider lock-in bandwidths at higher Reynolds number region. The cylindrical bluff body was found to generate the highest average power and determined to be the optimal bluff body for VIV harvester. For a cylindrical-bluff-body harvester with a beam length of 0.04m and a diameter of 0.02m at Re range of 300 to 1100, a maximum power of 0.35mW was numerically predicted.

Pobering and Schwesinger (2008) proposed a VIV energy harvester and investigated its behavior with CFD simulations. The development of von Kármán's vortex streets behind three cantilivers that were linearly arranged in a row. It was found that the upstream vortices from the prior cantilivers combine with and amplify the following ones, increasing the strain thus power generation capability of the downstream harvester. It can be inferred from this finding that by properly arranging a series of harvesters, the performance of VIV harvesters can be enhanced. Pobering, Menacher *et al.* (2009) also conducted CFD simulations to investigate the effect of bluff body shape on the performance of energy harvesters based on VIV. Cylindrical, triangular and hexagonal shapes were considered. Unlike the conclusion of Sivadas and Wickenheiser (2011), it was pointed out that the shape with a very sharp tear-off-edge like the triangular shape gage the best results in terms of the periodicity of vortices and value of the low pressure in the downstream air. The COMSOL Multiphysics software was employed for both studies.

Hobeck, Geslain *et al.* (2014) reported the phenomenon of dual cantilever flutter (DCF) during wind tunnel experiments, where two identical cantilivers underwent large amplitude and persistent vibrations when subject to wind flows. They proposed the first documented energy harvesting device based on this DCF phenomenon which consisted of two identical piezoelectric cantilivers. It was inferred that dynamics of one beam affected dynamics of the other through fluid coupling. CFD simulations were conducted using shear stress transport (SST) turbulence model with the ANSYS-CFX software for two types of dynamics, i.e., the entrainment dynamics and the flutter dynamics. The former means that when there is no flow, disturbance-induced vibration of one beam will cause the other beam to start to oscillate; while the later means the constant and identical amplitude but out of phase oscillations of the two beams during DCF. The meshing zone layouts are shown in Fig. 18, with the left and right graphs indicating the case without and with relative deflections, respectively. A non-conformal interface was used to separate the two beams into completely independent halves of fluid. The inlet and outlet in the left graph was changed to open like that in the right graph when modeling the entrainment dynamics. The CFD simulation results for entrainment dynamics successfully captured the experimental measurements. With two identical cantilivers of $14.6 \times 2.54 \times 0.0254$ cm^3, a maximum power of 0.796 mw was measured at around 13m/s. The performance of power generation was found sensitive to the gap distance. With smaller gap distances between 0.25 cm and 1.0 cm, it was found experimentally that the cantilivers produced a significant amount of power over a very large range of wind speeds from 3 m/s to 15 m/s. This is a great advantage of the DCF harvester.

Akaydin, Elvin *et al.* (2010a) employed FLUENT to conduct CFD simulations for their cantilevered harvester that can harvest energy from highly unsteady wind flows. Vortex shedding of an upstream cylinder was chosen to generate the desired unsteady turbulent flow. The shear stress transport (SST) k-ω turbulence model was employed during simulation. The meshing details are shown in the lower graph in Fig. 19. It can be seen that triangular cells were used in the vicinity of the beam in order to facilitate simple dynamic re-meshing at each time step; while in other areas including the cylinder area quadrilateral cells were used. High mesh density was used in the boundary layers in order to accurately model the viscous effects like vorticity generation. The cantilever with PVDF attached as the top layer underwent oscillations with relatively large amplitude of tip displacement and high operational frequency. Therefore, the shape of the piezoelectric generator was calculated at each predefined time step Δt and the boundary conditions thus the meshes were updated at each step.

CFD simulations have also been conducted to characterize the power harvesting from their VIV energy harvester by Mehmood, Abdelkefi *et al.* (2013), from a flutter-based electromagnetic harvester by Park, Morgenthal *et al.* (2014) and from a small-scale wind energy portable turbine by Kishore, Coudron *et al.* (2013). CFD simulation owns its advantage in giving clear visual observations of flow pressure distribution and structural deflection during the operation of an energy harvester, but it requires significant efforts in developing and updating meshes and tremendously high simulation time. To shorten the simulation time, in the above mentioned studies the CFD simulations were all conducted with 2D dimensions. Moreover, all the above mentioned CFD simulations in energy harvesting studies solved for the responses in the fluid and structure domains, however, components in the electrical domain, like the external load or more complex interface circuits, were not considered. The backward electromechanical coupling effect was either considered separately in the later data process or simplified into damping effect in the simulation. The fluid and mechanical responses were able to be directly obtained through CFD,

Table 2 Merits, demerits and applicable circumstances of different modeling methods for small-scale wind energy harvesting

Modeling methods	Merits, demerits, and applicable circumstances
Mathematical modeling	• Clear relationships for electromechanical coupling and fluid-structure coupling behaviors • Enable the derivation of explicit final mechanical and electrical response expressions • Fast evaluation of a harvesting system's performance • Efficient parameter optimization • Theoretical formulation is cumbersome if complex interface with nonlinear electronic components get involved
Equivalent circuit modeling	• Enable system-level circuit simulation by representing the aerodynamic and mechanical components with equivalent electronic components • Suitable for the case with practical interfaces with nonlinear power extraction process • Require additional finite element analyses to identify parameters for the case with complex mechanical structures
Computational fluid dynamics	• Give clear visual observations of flow pressure distribution and structural deflection • Give accurate responses in the fluid and structure domains • Enable simulation under complex flow conditions, like those with atmospheric turbulence or "gusts" • Backward electromechanical coupling and effects of the electronic interface have to be considered separately in later data process, or simplified into damping effect • Preferable for systems with complex mechanical structures

which were further employed as an input to derive the corresponding electrical response via circuit simulation or analytical calculation of the circuit governing equation.

7. Conclusions

This paper presents the fundamentals of small-scale wind energy harvesting techniques and detailed reviews of the state-of-the-art modeling methods. The mechanisms and characteristics of different types of aeroelastic instabilities, based on which wind energy harvesting systems operate, are presented, including the vortex-induced vibration, galloping, flutter, wake galloping and turbulence-induced vibration. The modeling methods of small-scale wind energy harvesters in the literature are generally classified into three categories: the mathematical modeling method, the equivalent circuit modeling method, and the computational fluid dynamics (CFD) method. The mathematical modeling is illustrated from two aspects, i.e., the electromechanical modeling part and the aerodynamic modeling part.

Theoretical analyses with the mathematical models establish clear relationships between the multi-way coupling and final mechanical and electrical responses, enabling fast evaluation of the harvester's performance and efficient parameter optimization. For the case with a simple AC circuit that consists of only a resistive load, the mathematical is easy and convenient to be utilized. For the case with complex interface circuits for AC-DC signal rectification and regulation, the coupling behaviors are further complicated due to the added nonlinear electronic components. To derive the theoretical responses of such systems, careful analyses of the energy flow patterns and energy balances in the system are required. For example, using the mathematical model, the mechanical and electrical responses of a galloping piezoelectric energy harvester integrated with a synchronized charge extraction (SCE) circuit are explicitly derived by Zhao and Yang (2015b)

based on the energy balances in the system. Yet for some cases, the power extraction interface is very complex and the theoretical formulations are too cumbersome to be developed. In such cases, the equivalent circuit modeling is greatly advantageous by representing the aerodynamic and mechanical components with equivalent electronic components, and enabling system-level simulation with the overall system circuit model. But it has to be noted that, if the mechanical structure of the harvester is complex, additional efforts are required to identify the analogical circuit parameters using finite element analysis. Computational fluid dynamics gives visualized interactions between the flow domain and the harvester structure domain. When the harvester's structure is complex, CFD will provide the most accurate fluid-structure interaction results. However, the backward electromechanical coupling as well as the effects of external load on system responses are not able to be integrated simultaneously and need to be considered separately. If more complex interfaces are employed, like the nonlinear power extraction circuit with synchronized switching feature, the situation will be even more troublesome. Future work on developing integrated multi-way coupling CFD model is desired. Obviously, there are other modeling issues that are not included in this review paper due to the length limit, such as the consideration of piezoelectric nonlinearity in the electromechanical model (Stanton, Erturk *et al.* 2010, Abdelkefi, Nayfeh *et al.* 2012a), and the consideration of effects of atmospheric turbulence or "gusts" in the aerodynamic model (Dowell 2015, Novak and Tanaka 1974, Xiang, Wu *et al.* 2015). To choose the suitable modeling method for a wind energy harvester, one has to consider comprehensively the multiple factors like whether a pure resistor load is considered in the circuit or nonlinear electronic components are involved, whether the mechanical structure is complex, and whether the unsteady aerodynamic effects can be ignored, etc. Moreover, although the above mentioned models can be independently employed, there is always the option of integrating two or

more of them to achieve better response predictions in certain scenarios. For example, for a harvester with complex structure and subjected to nonuniform flows, we can obtain the aerodynamic force using CFD and then introduce it into the mathematical model for further electromechanically coupled analysis. The merits, demerits as well as the applicable circumstances of the reviewed methods are summarized in Table 2.

Through this review article, the authors hope to provide some useful guidance for researchers from different disciplines who are interested to develop and model a wind energy harvester. Future improvement in the multi-way coupled wind energy harvesting modeling techniques will facilitate the development of integrated wind powered devices, like self-powered wireless sensors, and help lead the lab research to real engineering applications like civil and infrastructure health monitoring systems.

References

Abdelkefi, A. (2012), "Global nonlinear analysis of piezoelectric energy harvesting from ambient and aeroelastic vibrations", *Ph.D. Dissertation*, Virginia Polytechnic Institute and State University.

Abdelkefi, A. (2016), "Aeroelastic energy harvesting: A review", *IJES*, **100**, 112-135.

Abdelkefi, A. and Hajj, M.R. (2013), "Performance enhancement of wing-based piezoaeroelastic energy harvesting through freeplay nonlinearity", *Theor. Appl. Mech. Lett.*, **3**(4), 041001.

Abdelkefi, A., Hajj M.R. and Nayfeh A.H. (2012a), "Sensitivity analysis of piezoaeroelastic energy harvesters", *J. Intel. Mat. Syst. Str.*, **23**(13), 1523-1531.

Abdelkefi, A., Hajj M.R. and Nayfeh A.H. (2012b), "Phenomena and modeling of piezoelectric energy harvesting from freely oscillating cylinders", *Nonlinear Dynam.*, **70**(2), 1377-1388.

Abdelkefi, A., Hajj, M.R. and Nayfeh, A.H. (2012c), "Power harvesting from transverse galloping of square cylinder", *Nonlinear Dynam.*, **70**(2), 1355-1363.

Abdelkefi, A., Hajj, M.R. and Nayfeh, A.H. (2013d), "Piezoelectric energy harvesting from transverse galloping of bluff bodies", *Smart Mater. Struct.*, **22**(1), 015014.

Abdelkefi, A., Nayfeh, A. and Hajj, M. (2012a), "Effects of nonlinear piezoelectric coupling on energy harvesters under direct excitation", *Nonlinear Dynam.*, **67**(2), 1221-1232.

Abdelkefi, A., Nayfeh, A.H. and Hajj, M.R. (2012b), "Modeling and analysis of piezoaeroelastic energy harvesters", *Nonlinear Dynam.*, **67**(2), 925-939.

Abdelkefi, A., Nayfeh, A.H. and Hajj, M.R. (2012c), "Design of piezoaeroelastic energy harvesters", *Nonlinear Dynam.*, **68**(4), 519-530.

Abdelkefi, A., Nayfeh, A.H. and Hajj M.R. (2012d), "Enhancement of power harvesting from piezoaeroelastic systems", *Nonlinear Dynam.*, **68**(4), 531-541.

Abdelkefi, A., Scanlon, J.M., Mcdowell, E. and Hajj, M.R. (2013), "Performance enhancement of piezoelectric energy harvesters from wake galloping", *Appl. Phys. Lett.*, **103**(3), 033903.

Abdelkefi, A., Vasconcellos, R., Marques, F.D. and Hajj, M.R. (2012d), "Bifurcation analysis of an aeroelastic system with concentrated nonlinearities", *Nonlinear Dynam.*, **69**(1-2), 57-70.

Abdelkefi, A., Yan, Z. and Hajj, M.R. (2013b), "Modeling and nonlinear analysis of piezoelectric energy harvesting from transverse galloping", *Smart Mater. Struct.*, **22**(2), 025016.

Akaydin, H.D. (2012), "Piezoelectric energy harvesting from fluid flow", *Ph.D. Dissertation*, City University of New York.

Akaydin, H.D., Elvin, N. and Andreopoulos, Y. (2010a), "Energy harvesting from highly unsteady fluid flows using piezoelectric materials", *J. Intel. Mat. Syst. Str.*, **21**(13), 1263-1278.

Akaydın, H.D., Elvin, N. and Andreopoulos, Y. (2010b), "Wake of a cylinder: a paradigm for energy harvesting with piezoelectric materials", *Exp. Fluids*, **49**(1), 291-304.

Akaydın, H.D., Elvin, N. and Andreopoulos, Y. (2012), "The performance of a self-excited fluidic energy harvester", *Smart Mater. Struct.*, **21**(2), 025007.

ANSYS CFX. Retrieved December 10, 2014, from http://www.ansys.com/Products/Simulation+Technology/Fluid+Dynamics/Fluid+Dynamics+Products/ANSYS+CFX

ANSYS Fluent. Retrieved December 10, 2014, from http://www.ansys.com/Products/Simulation+Technology/Fluid+Dynamics/Fluid+Dynamics+Products/ANSYS+Fluent

Anton, S.R. and Sodano, H.A. (2007), "A review of power harvesting using piezoelectric materials (2003–2006)", *Smart Mater. Struct.*, **16**(3), 1-21.

Au-Yang, M.K. (2001), *Flow-induced vibration of power and process plant components : a practical workbook* (1st ed.), ASME Press, New York, NY.

Balakrishnan, A.V. (2012), *Aeroelasticity-Continuum Theory*, Springer-Verlag New York, New York, NY.

Balasubramanian, S., Skop, R., Haan, F. and Szewczyk, A. (2000), "Vortex-excited vibrations of uniform pivoted cylinders in uniform and shear flow", *JFS*, **14**(1), 65-85.

Bansal, A., Howey, D. and Holmes, A. (2009), "CM-scale air turbine and generator for energy harvesting from low-speed flows", *Proceedings of the Solid-State Sensors, Actuators and Microsystems Conference, 2009. TRANSDUCERS 2009. International.*

Barrero-Gil, A., Alonso, G. and Sanz-Andres, A. (2010), "Energy harvesting from transverse galloping", *J. Sound Vib.*, **329**(14), 2873-2883.

Barrero-Gil, A., Pindado, S. and Avila, S. (2012), "Extracting energy from Vortex-Induced Vibrations: A parametric study", *Appl. Math. Modell.*, **36**(7), 3153-3160.

Beeby, S.P., Tudor, M.J. and White, N.M. (2006), "Energy harvesting vibration sources for microsystems applications", *Meas. Sci. Technol.*, **17**(12), 175-195.

Bibo, A. (2014), "Investigation of concurrent energy harvesting from ambient vibrations and wind", *Ph.D. Dissertation*, Clemson University.

Bibo, A. and Daqaq, M.F. (2013a), "Energy harvesting under combined aerodynamic and base excitations", *J. Sound Vib.*, **332**(20), 5086-5102.

Bibo, A. and Daqaq, M.F. (2013b), "Investigation of concurrent energy harvesting from ambient vibrations and wind using a single piezoelectric generator", *Appl. Phys. Lett.*, **102**(24), 243904.

Bibo, A. and Daqaq, M.F. (2014), "On the optimal performance and universal design curves of galloping energy harvesters", *Appl. Phys. Lett.*, **104**(2), 023901.

Bibo, A., Abdelkefi, A. and Daqaq, M.F. (2015), "Modeling and characterization of a piezoelectric energy harvester under combined aerodynamic and base excitations", *J. Vib. Acoust.*, **137**(3), 031017.

Bibo, A., Alhadidi, A.H. and Daqaq. M.F. (2015), "Exploiting a nonlinear restoring force to improve the performance of flow energy harvesters", *J. Appl. Phys.*, **117**(4), 045103.

Bressers, S., Avirovik, D., Lallart, M., Inman, D.J. and Priya, S. (2011), *Contact-less Wind Turbine Utilizing Piezoelectric Bimorphs with Magnetic Actuation*, Springer, New York.

Bressers, S., Vernier, C., Regan, J., Chappell, S., Hotze, M., Luhman, S., Avirovik, D. and Priya, S. (2010), "Small-scale modular wind turbine", *Proceedings of SPIE*, 764333.

Bryant, M. (2012), "Aeroelastic flutter vibration energy harvesting:

modeling, testing, and system eesign", *Ph.D. Dissertation*, Cornell University.

Bryant, M. and Garcia, E. (2009), "Energy harvesting: a key to wireless sensor nodes", *Proceedings of the 2nd International Conference on Smart Materials and Nanotechnology in Engineering*, 74931W.

Bryant, M. and Garcia, E. (2011), "Modeling and testing of a novel aeroelastic flutter energy harvester", *J. Vib. Acoust.*, **133**(1), 011010.

Bryant, M., Pizzonia, M., Mehallow, M. and Garcia, E. (2014), "Energy harvesting for self-powered aerostructure actuation", *Proceedings of SPIE*, 90570E.

Bryant, M., Schlichting, A.D. and Garcia, E. (2013), "Toward efficient aeroelastic energy harvesting: device performance comparisons and improvements through synchronized switching", *Proceedings of SPIE*, 868807.

Bryant, M., Shafer, M.W. and Garcia, E. (2012), "Power and efficiency analysis of a flapping wing wind energy harvester", *Proceedings of SPIE*, 83410E

Bryant, M., Tse, R. and Garcia, E. (2012), "Investigation of host structure compliance in aeroelastic energy harvesting", *Proceedings of the ASME 2012 Conference on Smart Materials, Adaptive Structures and Intelligent Systems*.

Bryant, M., Wolff, E. and Garcia, E. (2011), "Parametric design study of an aeroelastic flutter energy harvester", *Proceedings of SPIE*, 79770S.

Castagnetti, D. (2012), "Experimental modal analysis of fractal-inspired multi-frequency structures for piezoelectric energy converters", *Smart Mater. Struct.*, **21**(9), 094009.

Chen, C.T., Islam, R.A. and Priya, S. (2006), "Electric energy generator", *IEEE T. Ultrason. Ferr.*, **53**(3), 656-661.

Chen, W.C. (1993), "A formulation of nonlinear limit cycle oscillation problems in aircraft flutter", *Master Dissertation*, Massachusetts Institute of Technology.

Computational fluid dynamics, Wikipedia. Retrieved December 10, 2014, from http://en.wikipedia.org/wiki/Computational_fluid_dynamics

COMSOL CFD Module. Retrieved December 10, 2014, from http://www.comsol.com/cfd-module

Cook-Chennault, K., Thambi, N. and Sastry, A. (2008), "Powering MEMS portable devices—a review of non-regenerative and regenerative power supply systems with special emphasis on piezoelectric energy harvesting systems", *Smart Mater. Struct.*, **17**(4), 043001.

Dai, H., Abdelkefi, A., Javed, U. and Wang, L. (2015), "Modeling and performance of electromagnetic energy harvesting from galloping oscillations", *Smart Mater. Struct.*, **24**(4), 045012.

Dai, H.L., Abdelkefi, A. and Wang, L. (2014a), "Theoretical modeling and nonlinear analysis of piezoelectric energy harvesting from vortex-induced vibrations", *J. Intel. Mat. Syst. Str.*, **25**(14), 1861-1874.

Dai, H.L., Abdelkefi, A. and Wang, L. (2014b), "Piezoelectric energy harvesting from concurrent vortex-induced vibrations and base excitations", *Nonlinear Dynam.*, **77**(3), 967-981.

Daqaq, M.F., Masana, R., Erturk, A. and Quinn, D.D. (2014), "On the role of nonlinearities in vibratory energy harvesting: a critical review and discussion", *ApMRv*, **66**(4), 040801.

Dat, R. and Tran, C. (1981), "Investigation of the stall flutter of an airfoil with a semi-empirical model of 2 D flow", *ONERA, TP no. 1981-146, 1981. 11 p.*

De Marqui, C. and Erturk A. (2012), "Electroaeroelastic analysis of airfoil-based wind energy harvesting using piezoelectric transduction and electromagnetic induction", *J. Intel. Mat. Syst. Str.*, **24**(7), 846-854.

De Marqui, C., Erturk, A. and Inman, D.J. (2010), "Piezoaeroelastic modeling and analysis of a generator wing with continuous and segmented electrodes", *J. Intel. Mat. Syst.*

Str., **21**(10), 983-993.

Den Hartog, J.P. (1956), *Mechanical Vibrations*, New York: McGraw-Hill.

Dowell, E. (2015), *A Modern Course in Aeroelasticity*, Springer International Publishing.

Dowell, E., Edwards, J. and Strganac, T. (2003), "Nonlinear aeroelasticity", *JAir*, **40**(5), 857-874.

Dugundji, J. (1992), "Nonlinear problems of aeroelasticity", *Comput. Nonlinear Mech, Aerospace Eng.*, **1**, 127-155.

Dunn, P. and Dugundji, J. (1992), "Nonlinear stall flutter and divergence analysis of cantilevered graphite/epoxy wings", *AIAA J.*, **30**(1), 153-162.

Dutoit, N.E., Wardle, B.L. and Kim, S.G. (2005), "Design considerations for mems-scale piezoelectric mechanical vibration energy harvesters", *InFer*, **71**(1), 121-160.

El-Hami, M., Glynne-Jones, P., White, N., Hill, M., Beeby, S., James, E., Brown, A. and Ross, J. (2001), "Design and fabrication of a new vibration-based electromechanical power generator", *Sensor. Actuat. A. –Phys.*, **92**(1), 335-342.

Elvin, N.G. (2014), "Equivalent electrical circuits for advanced energy harvesting", *J. Intel. Mat. Syst. Str.*, **25**(14), 1715-1726.

Elvin, N.G. and Elvin, A.A. (2009a), "A general equivalent circuit model for piezoelectric generators", *J. Intel. Mat. Syst. Str.*, **20**(1), 3-9.

Elvin, N.G. and Elvin, A.A. (2009b), "A coupled finite element—circuit simulation model for analyzing piezoelectric energy generators", *J. Intel. Mat. Syst. Str.*, **20**(5), 587-595.

Elvin, N.G. and Elvin, A.A. (2011), "An experimentally validated electromagnetic energy harvester", *J. Sound Vib.*, **330**(10), 2314-2324.

Erturk, A. (2009), "Electromechanical modeling of piezoelectric energy harvesters", *Ph.D. Dissertation*, Virginia Polytechnic Institute and State University.

Erturk, A. and Inman, D.J. (2008a), "A distributed parameter electromechanical model for cantilevered piezoelectric energy harvesters", *J. Vib. Acoust.*, **130**(4), 041002.

Erturk, A. and Inman, D.J. (2008b), "On mechanical modeling of cantilevered piezoelectric vibration energy harvesters", *J. Intel. Mat. Syst. Str.*, **19**(11), 1311-1325.

Erturk, A., Vieira, W., De Marqui, Jr C. and Inman, D. (2010), "On the energy harvesting potential of piezoaeroelastic systems", *Appl. Phys. Lett.*, **96**(18), 184103.

Ewere, F., Wang, G. and Cain, B. (2014), "Experimental investigation of galloping piezoelectric energy harvesters with square bluff bodies", *Smart Mater. Struct.*, **23**(10), 104012.

Facchinetti, M.L., De Langre, E. and Biolley, F. (2002), "Vortex shedding modeling using diffusive van der Pol oscillators", *Comptes Rendus Mecanique*, **330**(7), 451-456.

Facchinetti, M.L., De Langre, E. and Biolley, F. (2004), "Coupling of structure and wake oscillators in vortex-induced vibrations", *JFS*, **19**(2), 123-140.

Federspiel, C.C. and Chen, J. (2003), "Air-powered sensor", *Proceedings of Sensors, 2003. Proceedings of IEEE*, 22-25.

Fung, Y.C. (1955), *An introduction to the theory of aeroelasticity*, John Wiley, New York, NY.

Global wind energy council, wind in numbers. Retrieved November 4, 2014, from http://www.gwec.net/global-figures/wind-in-numbers/

Glynne-Jones, P., Tudor, M., Beeby, S. and White, N. (2004), "An electromagnetic, vibration-powered generator for intelligent sensor systems", *Sensor. Actuat. A - Phys.*, **110**(1), 344-349.

Gomez, J.C., Bryant, M. and Garcia, E. (2014), "Low-order modeling of the unsteady aerodynamics in flapping wings", *JAir*, 1-10.

Harne, R. and Wang, K. (2013), "A review of the recent research on vibration energy harvesting via bistable systems", *Smart Mater. Struct.*, **22**(2), 023001.

Hobbs, W.B. and Hu, D.L. (2012), "Tree-inspired piezoelectric energy harvesting", *JFS*, **28**, 103-114.

Hobeck, J.D. and Inman, D. (2012a), "Design and analysis of dual pressure probes for predicting turbulence-Induced vibration in low velocity flow", *Proceedings of the 53rd AIAA/ASME/ASCE/AHS/ASC Structures, Structural Dynamics, and Materials Conference*.

Hobeck, J.D. and Inman, D.J. (2012b), "Artificial piezoelectric grass for energy harvesting from turbulence-induced vibration", *Smart Mater. Struct.*, **21**(10), 105024.

Hobeck, J.D. (2014), "Energy harvesting with piezoelectric grass for autonomous self-sustaining sensor networks", *Ph.D. Dissertation*, The University of Michigan.

Hobeck, J.D. and Inman, D.J. (2014), "A distributed parameter electromechanical and statistical model for energy harvesting from turbulence-induced vibration", *Smart Mater. Struct.*, **23**(11), 115003.

Hobeck, J.D., Geslain, D. and Inman, D.J. (2014), "The dual cantilever flutter phenomenon: a novel energy harvesting method", *Proceedings of SPIE*, 906113.

Hodges, D.H. and Pierce, G.A. (2002), *Introduction to Structural Dynamics and Aeroelasticity* (Vol. 15), Cambridge University Press.

Howey, D., Bansal, A. and Holmes, A. (2011), "Design and performance of a centimetre-scale shrouded wind turbine for energy harvesting", *Smart Mater. Struct.*, **20**(8), 085021.

Huang, L. (1995), "Flutter of cantilevered plates in axial flow", *JFS*, **9**(2), 127-147.

Humdinger Wind Energy, Windbelt Innovation. Retrieved November 7, 2014, from http://www.humdingerwind.com

Jeon, Y., Sood, R., Jeong, J.H. and Kim, S.G. (2005), "MEMS power generator with transverse mode thin film PZT", *Sensor. Actuat. A. – Phys.*, **122**(1), 16-22.

Jones, K.D., Davids, S. and Platzer, M.F. (1999), "Oscillating-wing power generator", *Proceedings of the ASME/JSME joint fluids engineering conference*.

Jung, H.J. and Lee, S.W. (2011), "The experimental validation of a new energy harvesting system based on the wake galloping phenomenon", *Smart Mater. Struct.*, **20**(5), 055022.

Karami, M.A. (2012), "Micro-scale and nonlinear vibrational energy harvesting", *Ph.D. Dissertation*, Virginia Polytechnic Institute and State University.

Karami, M.A., Farmer, J.R. and Inman, D.J. (2013), "Parametrically excited nonlinear piezoelectric compact wind turbine", *Renew. Energ.*, **50**, 977-987.

Kim, H.S., Kim, J.H. and Kim, J. (2011), "A review of piezoelectric energy harvesting based on vibration", *Int. J. Precision Eng. Manufact.*, **12**(6), 1129-1141.

Kishore, R.A., Coudron, T. and Priya, S. (2013), "Small-scale wind energy portable turbine (SWEPT)", *J. Wind Eng. Ind. Aerod.*, **116**, 21-31.

Kwon, S.D. (2010), "A T-shaped piezoelectric cantilever for fluid energy harvesting", *Appl. Phys. Lett.*, **97**(16), 164102.

Lallart, M. and Guyomar, D. (2008), "An optimized self-powered switching circuit for non-linear energy harvesting with low voltage output", *Smart Mater. Struct.*, **17**(3), 035030.

Lee, B., Price, S. and Wong, Y. (1999), "Nonlinear aeroelastic analysis of airfoils: bifurcation and chaos", *PrAeS*, **35**(3), 205-334.

Lefeuvre, E., Badel, A., Richard, C. and Guyomar, D. (2007), "Energy harvesting using piezoelectric materials: Case of random vibrations", *J. Electroceram.*, **19**(4), 349-355.

Lefeuvre, E., Badel, A., Richard, C., Petit, L. and Guyomar, D. (2006), "A comparison between several vibration-powered piezoelectric generators for standalone systems", *Sensors Actuat. A: Phys.*, **126**(2), 405-416.

Li, F., Xiang, T., Chi, Z., Luo, J., Tang, L., Zhao, L. and Yang, Y. (2013), "Powering indoor sensing with airflows: a trinity of energy harvesting, synchronous duty-cycling, and sensing", *Proceedings of the 11th ACM Conference on Embedded Networked Sensor Systems*.

Liang, J. and Liao, W.H. (2012), "Improved design and analysis of self-powered synchronized switch interface circuit for piezoelectric energy harvesting systems", *ITIE*, **59**(4), 1950-1960.

Lien, I.C., Shu, Y.C., Wu, W.J., Shiu, S.M. and Lin, H.C. (2010), "Revisit of series-SSHI with comparisons to other interfacing circuits in piezoelectric energy harvesting", *Smart Mater. Struct.*, **19**(12), 125009.

Lu, F., Lee, H. and Lim, S. (2004), "Modeling and analysis of micro piezoelectric power generators for micro-electromechanical-systems applications", *Smart Mater. Struct.*, **13**(1), 57.

Mahajan, A.J., Kaza, K.R. and Dowell, E. (1993), "Semi-empirical model for prediction of unsteady forces on an airfoil with application to flutter", *JFS*, **7**(1), 87-103.

McAlister, K.W., Lambert, O. and Petot, D. (1984), "Application of the ONERA model of dynamic stall", *DTIC Document*, No. NASA-A-9824.

McCarthy, J.M., Watkins, S., Deivasigamani, A. and John, S.J. (2016), "Fluttering energy harvesters in the wind: A review", *J. Sound Vib.*, **361**, 355-377.

McKinney, W. and Delaurier, J. (1981), "Wingmill: an oscillating-wing windmill", *JEner*, **5**(2), 109-115.

Mehmood, A., Abdelkefi, A., Hajj, M.R., Nayfeh, A.H., Akhtar, I. and Nuhait, A.O. (2013), "Piezoelectric energy harvesting from vortex-induced vibrations of circular cylinder", *J. Sound Vib.*, **332**(19), 4656-4667.

Meninger, S., Mur-Miranda, J.O., Amirtharajah, R., Chandrakasan, A.P. and Lang, J.H. (2001), "Vibration-to-electric energy conversion", *IEEE T. Very Large Scale Integration (VLSI) Systems*, **9**(1), 64-76.

Mitcheson, P.D., Miao, P., Stark, B.H., Yeatman, E., Holmes, A. and Green, T. (2004), "MEMS electrostatic micropower generator for low frequency operation", *Sensors Actuat. A: Phys.*, **115**(2), 523-529.

Myers, R., Vickers, M., Kim, H. and Priya, S. (2007), "Small scale windmill", *Appl. Phys. Lett.*, **90**(5), 054106.

Novak, M. (1969), "Aeroelastic galloping of prismatic bodies", *J. Eng. Mech. Div. - ASCE*, **95**, 115-142.

Novak, M. and Tanaka, H. (1974), "Effect of turbulence on galloping instability", *J. Eng. Mech. - ASCE* **100**(1), 27-47.

Païdoussis, M.P., Price, S.J. and De Langre, E. (2010), *Fluid-structure interactions: Cross-flow-induced instabilities*, Cambridge University Press, New York.

Park, J., Morgenthal, G., Kim, K., Kwon, S.D. and Law, K.H. (2014), "Power evaluation of flutter-based electromagnetic energy harvesters using computational fluid dynamics simulations", *J. Intel. Mat. Syst. Str.*, **25**(14), 1800-1812.

Park, J.W., Jung, H.J., Jo, H. and Spencer, B.F. (2012), "Feasibility study of micro-wind turbines for powering wireless sensors on a cable-stayed bridge", *Energies*, **5**(9), 3450-3464.

Pellegrini, S.P., Tolou, N., Schenk, M. and Herder, J.L. (2013), "Bistable vibration energy harvesters: A review", *J. Intel. Mat. Syst. Str.*, **24**(11), 1303-1312.

Peters, D.A. (1985), "Toward a unified lift model for use in rotor blade stability analyses", *J. Am. Helicopter Soc.*, **30**(3), 32-42.

Peters, D.A., Karunamoorthy, S. and Cao, W.M. (1995), "Finite state induced flow models. I-Two-dimensional thin airfoil", *JAir*, **32**(2), 313-322.

Piezoelectric materials. Retrieved November 4, 2014, from http://www.piezomaterials.com/

Pobering, S. and Schwesinger, N. (2008), "Power supply for wireless sensor systems", *Proceedings of Sensors, 2008 IEEE*,

685-688.

Pobering, S., Menacher, M., Ebermaier, S. and Schwesinger, N. (2009), "Piezoelectric power conversion with self-induced oscillation", *Proceedings of PowerMEMS*, 384-387.

Powell, A. (1958), "On the fatigue failure of structures due to vibrations excited by random pressure fields", *J. Acoust. Soc. Am.*, **30**(12), 1130-1135.

Priya, S. (2005), "Modeling of electric energy harvesting using piezoelectric windmill", *Appl. Phys. Lett.*, **87**(18), 184101.

Priya, S., Chen, C.T., Fye, D. and Zahnd, J. (2005), "Piezoelectric windmill: A novel solution to remote sensing", *Jpn. J. Appl. Phys.*, **44**(3), 104-107.

Rancourt, D., Tabesh, A. and Fréchette, L.G. (2007), "Evaluation of centimeter-scale micro windmills: aerodynamics and electromagnetic power generation", *Proceedings of PowerMEMS*, 93-96.

Roundy, S. and Wright, P.K. (2004), "A piezoelectric vibration based generator for wireless electronics", *Smart Mater. Struct.*, **13**(5), 1131-1142.

Roundy, S., Wright, P.K. and Rabaey, J. (2003), "A study of low level vibrations as a power source for wireless sensor nodes", *Comput. Commun.*, **26**(11), 1131-1144.

Ruscheweyh, H. (1983), "Aeroelastic interference effects between slender structures", *J. Wind Eng. Ind. Aerod.*, **14**(1), 129-140.

Sarpkaya, T. (2004), "A critical review of the intrinsic nature of vortex-induced vibrations", *JFS*, **19**(4), 389-447.

Schmidt, V.H. (1985), US4536674 A.

Schmidt, V.H. (1992), "Piezoelectric energy conversion in windmills", *Proceedings of Ultrasonics Symposium, IEEE 1992*, 897-904.

Shiraishi, N., Matsumoto, M. and Shirato, H. (1986), "On aerodynamic instabilities of tandem structures", *J. Wind Eng. Ind. Aerod.*, **23**, 437-447.

Sirohi, J. and Mahadik, R. (2011), "Piezoelectric wind energy harvester for low-power sensors", *J. Intel. Mat. Syst. Str.*, **22**(18), 2215-2228.

Sirohi, J. and Mahadik, R. (2012), "Harvesting wind energy using a galloping piezoelectric beam", *J. Vib. Acoust.*, **134**(1), 011009.

Sivadas, V. and Wickenheiser, A.M. (2011), "A study of several vortex-induced vibration techniques for piezoelectric wind energy harvesting", *Proceedings of SPIE*, 79770F.

Sodano, H.A., Park, G. and Inman, D.J. (2004), "An investigation into the performance of macro-fiber composites for sensing and structural vibration applications", *MSSP*, **18**(3), 683-697.

Sorribes-Palmer, F. and Sanz-Andres, A. (2013), "Optimization of energy extraction in transverse galloping", *JFS*, **43**, 124-144.

Sousa, V., De M Anicézio, M., De Marqui Jr., C. and Erturk, A. (2011), "Enhanced aeroelastic energy harvesting by exploiting combined nonlinearities: theory and experiment", *Smart Mater. Struct.*, **20**(9), 094007.

Stanton, S.C., Erturk, A., Mann, B.P. and Inman, D.J. (2010), "Nonlinear piezoelectricity in electroelastic energy harvesters: modeling and experimental identification", *J. Appl. Phys.*, **108**(7), 074903.

Sterken, T., Fiorini, P., Baert, K., Borghs, G. and Puers, R. (2004), "Novel design and fabrication of a MEMS electrostatic vibration scavenger", *Proceedings of PowerMEMS* 18-21.

Strasser, M., Aigner, R., Lauterbach, C., Sturm, T., Franosch, M. and Wachutka, G. (2004), "Micromachined CMOS thermoelectric generators as on-chip power supply", *Sensors Actuat. A: Phys.*, **114**(2), 362-370.

Strganac, T.W., Ko, J. and Thompson, D.E. (2000), "Identification and control of limit cycle oscillations in aeroelastic systems", *J. Guid. Control, Dynam.*, **23**(6), 1127-1133.

Tang, D. and Dowell, E. (1996), "Comments on the ONERA stall aerodynamic model and its impact on aeroelastic stability", *JFS*, **10**(4), 353-366.

Tang, D.M., Yamamoto, H. and Dowell, E.H. (2003), "Flutter and limit cycle oscillations of two-dimensional panels in three-dimensional axial flow", *JFS*, **17**(2), 225-242.

Tang, L., Yang, Y. and Soh, C.K. (2010), "Toward broadband vibration-based energy harvesting", *J. Intel. Mat. Syst. Str.*, **21**(18), 1867-1897.

Tang, L., Zhao, L., Yang, Y. and Lefeuvre, E. (2015), "Equivalent circuit representation and analysis of galloping-based wind energy harvesting", *IEEE/ASME T. Mechatronics*, **20**, 834-844.

Theodorsen, T. (1934). General Theory of Aerodynamic Instability and the Mechanism of Flutter.

Tien, C.M.T. and Goo, N.S. (2010), "Use of a piezo-composite generating element for harvesting wind energy in an urban region", *Aircraft Eng. Aerospace Technol.*, **82**(6), 376-381.

Tokoro, S., Komatsu, H., Nakasu, M., Mizuguchi, K. and Kasuga, A. (2000), "A study on wake-galloping employing full aeroelastic twin cable model", *J. Wind Eng. Ind. Aerod.*, **88**(2), 247-261.

Torres, E.O. and Rincón-Mora, G.A. (2009), "Electrostatic energy-harvesting and battery-charging CMOS system prototype", *IEEE Transactions on Circuits and Systems I: Regular Papers*, **56**(9), 1938-1948.

Tran, C.T. and Petot, D. (1981), "Semi-empirical model for the dynamic stall of airfoils in view of application to the calculated responses of a helicopter in forward flight", *Vert*, **51**, 35-53.

Truitt, A. and Mahmoodi, S.N. (2013), "A review on active wind energy harvesting designs", *Int. J. Precision Eng. Manufact.*, **14**(9), 1667-1675.

Vestas V164-8.0 nacelle and hub. Retrieved November 4, 2014, from http://www.windpowermonthly.com/article/1211056/close---vestas-v164-80-nacelle-hub

Wang, Y. (2012), "Simultaneous energy harvesting and vibration control via piezoelectric materials", *Ph.D. Dissertation*, Virginia Polytechnic Institute and State University.

Wang, Z.L. (2011), *Nanogenerators for self-powered devices and systems*, Georgia Institute of Technology, Atlanta.

Weinstein, L.A., Cacan, M.R., So, P.M. and Wright, P.K. (2012), "Vortex shedding induced energy harvesting from piezoelectric materials in heating, ventilation and air conditioning flows", *Smart Mater. Struct.*, **21**(4), 045003.

Wickenheiser, A.M., Reissman, T., Wu, W.J. and Garcia, E. (2010), "Modeling the effects of electromechanical coupling on energy storage through piezoelectric energy harvesting", *IEEE/ASME T. Mechatronics*, **15**(3), 400-411.

Williams, C.B. and Yates, R.B. (1996), "Analysis of a micro-electric generator for microsystems", *Sensor. Actuat. A. –Phys.*, **52**(1-3), 8-11.

Williamson, C.H. (1996), "Vortex dynamics in the cylinder wake", *AnRFM*, **28**(1), 477-539.

Williamson, C.H.K. and Govardhan, R. (2004), "Vortex-induced vibrations", *AnRFM*, **36**(1), 413-455.

Xiang, J., Wu, Y. and Li, D. (2015), "Energy harvesting from the discrete gust response of a piezoaeroelastic wing: Modeling and performance evaluation", *J. Sound Vib.*, **343**, 176-193.

Xiang, J., Yan, Y. and Li, D. (2014), "Recent advance in nonlinear aeroelastic analysis and control of the aircraft", *ChJA*, **27**(1), 12-22.

Xiao, Q. and Zhu, Q. (2014), "A review on flow energy harvesters based on flapping foils", *JFS*, **46**, 174-191.

Xie, J., Yang, J., Hu, H., Hu, Y. and Chen, X. (2012), "A piezoelectric energy harvester based on flow-induced flexural vibration of a circular cylinder", *J. Intel. Mat. Syst. Str.*, **23**(2), 135-139.

Xu, F., Yuan, F., Hu, J. and Qiu, Y. (2010), "Design of a miniature wind turbine for powering wireless sensors", *Proceedings of SPIE*, 764741.

Yan, Z. and Abdelkefi, A. (2014), "Nonlinear characterization of concurrent energy harvesting from galloping and base excitations", *Nonlinear Dynam.*, **77**(4), 1171-1189.

Yang, Y. and Tang, L. (2009), "Equivalent circuit modeling of piezoelectric energy harvesters", *J. Intel. Mat. Syst. Str.*, **20**(18), 2223-2235.

Yang, Y., Zhao, L. and Tang, L. (2013), "Comparative study of tip cross-sections for efficient galloping energy harvesting", *Appl. Phys. Lett.*, **102**(6), 064105.

Zhao, L. (2015), "Small-scale wind energy harvesting using piezoelectric materials", *Ph.D. Dissertation*, Nanyang Technological University.

Zhao, L. and Yang, Y. (2015a), "Enhanced aeroelastic energy harvesting with a beam stiffener", *Smart Mater. Struct.*, **24**(3), 032001.

Zhao, L. and Yang, Y. (2015b), "Analytical solutions for galloping-based piezoelectric energy harvesters with various interfacing circuits", *Smart Mater. Struct.*, **24**(7), 075023.

Zhao, L. and Yang, Z. (1990), "Chaotic motions of an airfoil with non-linear stiffness in incompressible flow", *J. Sound Vib.*, **138**(2), 245-254.

Zhao, L., Liang, J., Tang, L., Yang, Y. and Liu, H. (2015), "Enhancement of galloping-based wind energy harvesting by synchronized switching interface circuits", *Proceedings of SPIE*, 943113.

Zhao, L., Tang, L. and Yang, Y. (2012), "Small wind energy harvesting from galloping using piezoelectric materials", *Proceedings of the ASME 2012 Conference on Smart Materials, Adaptive Structures and Intelligent Systems*.

Zhao, L., Tang, L. and Yang, Y. (2013), "Comparison of modeling methods and parametric study for a piezoelectric wind energy harvester", *Smart Mater. Struct.*, **22**(12), 125003.

Zhao, L., Tang, L. and Yang, Y. (2014a), "Enhanced piezoelectric galloping energy harvesting using 2 degree-of-freedom cut-out cantilever with magnetic interaction", *Jpn. J. Appl. Phys.*, **53**(6), 060302.

Zhao, L., Tang, L. and Yang, Y. (2016), "Synchronized charge extraction in galloping piezoelectric energy harvesting", *J. Intel. Mat. Syst. Str.*, **27**(4), 453-468.

Zhao, L., Tang, L., Wu, H. and Yang, Y. (2014b), "Synchronized charge extraction for aeroelastic energy harvesting", *Proceedings of SPIE*, 90570N.

Zhu, Q. (2011), "Optimal frequency for flow energy harvesting of a flapping foil", *J. Fluid Mech.*, **675**, 495-517.

Zhu, Q. and Peng, Z. (2009), "Mode coupling and flow energy harvesting by a flapping foil", *Physics of Fluids (1994-present)*, **21**(3), 033601.

Zhu, Q., Haase, M. and Wu, C.H. (2009), "Modeling the capacity of a novel flow-energy harvester", *Appl. Math. Model.*, **33**(5), 2207-2217.

CC